NASA Technical Memorandum 85804

Conceptual Design for Scaled Truss Antenna Flight Experiment

Wendell H. Lee

NOVEMBER 1984

NASA

NASA Technical Memorandum 85804

Conceptual Design for Scaled Truss Antenna Flight Experiment

Wendell H. Lee
Langley Research Center
Hampton, Virginia

NASA
National Aeronautics
and Space Administration
Scientific and Technical
Information Branch
1984

Contents

Symbols and Abbreviations

ASD	acceleration spectral density at f_n, g^2/Hz
A	cross-sectional area, m^2
a	solar absorptivity
BT	box truss
C	multiplication factor to obtain 97-percent confidence level
c	specific heat, kJ/kg-K
D	diameter, m
D_i	inside diameter, m
D_o	outside diameter, m
dx, dy, dz	normalized displacements, cm
EOS	Earth Observation Spacecraft
E	Young's modulus of elasticity, Pa
E_c	Young's modulus of elasticity for columns, Pa
e	thermal emittance
f	frequency, Hz
f_n	natural frequency of tube, Hz
f_p	frequency of plate vibration, Hz
f_t	frequency of truss vibration, Hz
Gr/E	graphite/epoxy
G_R	peak response acceleration (97-percent confidence level), g units
g	acceleration of gravity
IDEAS	Interactive Design and Evaluation of Advanced Spacecraft
$I, I_{XX}, I_{YY}, I_{ZZ}$	moments of inertia, kg-m^2
i	inclination, deg
LMSS	Land Mobile Satellite System
LSS	large space systems
L	length, m
ℓ	column member length, m
NSP	nondimensional scaling parameter
P	column load, N
Q_R	random dynamic magnification factor, 10 (conservative)
RMS	remote manipulator system
RF	radio frequency
SADE	Structural Assembly Demonstration Experiment
STAS	Scaled Truss Antenna Structure
STASEP	Scaled Truss Antenna Structures Experiment Program
STEP	Space Technology Experiments Platform
STS	Space Transportation System
S	bending stiffness, $Et^2/12(1-\nu^2)$
TT	tetrahedral truss
t	thickness, m
y	longitudinal distance
α	coefficient of thermal expansion, K^{-1}
β	angle between orbit normal vector and solar vector, deg
ν	Poisson's ratio
Π_1, Π_2, Π_3	nondimensional scaling parameters
ρ	density, kg/m^3
ρt	mass per unit area of plate material, kg/m^2
ρ_c	density of column material, kg/m^3
σ_{cr}	critical stress
ψ	angle between solar vector (Sun to Earth) and Y-axis (solar vector is always in X-Y plane), deg
Ω	angle in equatorial plane between solar vector at equinox and intersection of orbit plane with equatorial plane (line of nodes) when satellite is headed north, deg
ω	circular frequency
Subscripts:	
m	model
max	maximum
min	minimum
p	prototype

Introduction

With the Space Transportation System now operational, the capability for deploying and utilizing large space systems (LSS) exists. Consequently, development of qualified flight hardware for these systems is needed. The high degree of confidence in the flight readiness and reliability of current operational satellite systems is based on mature experience in technology, design, analyses, ground testing, flight experiments, and operational hardware. A high level of confidence in LSS systems requires similar specific experience, plus new developments in analysis techniques, design methods, static and dynamic structural measurements, packaging and deployment concepts, handling and testing, and materials.

Recent studies have proposed a number of LSS applications. Among them are the Earth Observation Spacecraft (EOS) and the Land Mobile Satellite System (LMSS). The EOS will be equipped with a complementary set of remote sensors for Earth, oceanic, and atmospheric observations of such items as atmospheric and sea surface temperatures, water pollutants, soil moisture, and land surface topography. The EOS structure will support a mesh antenna surface 120 by 60 m and a 116-m-long feed mast. One of the LMSS concepts proposes a satellite in geosynchronous orbit to provide mobile communications for commercial and government applications in nonmetropolitan areas of the continental United States. Depending on alternatives, single aperture or quad aperture, the antenna support structure should be 55 m or 122 m in diameter. The large size of these future spacecraft requires the application of nontraditional philosophies and techniques for establishing flight readiness. Size limitations of facilities preclude certain types of full-scale testing, such as thermal vacuum, far-field RF performance, and perhaps even deployment of the total structure. The $1g$ ground environment does not allow duplication of $0g$ orbit conditions; thus, exact testing is prevented in critical areas such as kinetics and structural dynamics, and the correlation and understanding of analysis techniques, scaling, structural dynamics, shape determination, and deployment are complicated. A bibliography of related work is included in this paper.

This paper describes the Scaled Truss Antenna Structures Experiment Program (STASEP) and defines the conceptual design of the Scaled Truss Antenna Structure (STAS). The objective of STASEP is to advance the knowledge and confidence level for producing flight-qualified LSS hardware. This objective will be accomplished by utilizing four subscale truss antenna structures to relate analyses, simulation, scaling, ground testing, and actual in-orbit performance of flight-type hardware. The building, launching, and operation of future LSS represent a large investment of resources, and the decisions to make these types of commitments must be based on sound knowledge of and experience with both theory and hardware. This goal probably will be best realized by multiple programs of relatively low risk and cost, which represent a greater number of more modest technical advances, rather than by a limited number of programs with the potential for greater payoff but with associated high risk and cost. The STASEP is a relatively modest program. Furthermore, it has the significant advantage of being able to provide quickly a large segment of worthwhile information prior to making a large commitment to the flight phase of the experiment.

Scaled Truss Antenna Structures Experiment Program

The basic STASEP flight hardware includes four truss structures mounted to the Space Technology Experiments Platform (STEP), which will be flown on the Shuttle. There are two types of truss structures, tetrahedral and box, and two sizes of each type, 6 m and 15 m. These scaled truss antenna structures will serve as pathfinders for larger structures by providing a basis for studies and correlations of scaling, simulation, structural characterization, and testing. In addition, the STASEP is an integral part of a broader technology development and verification program for LSS.

The Langley Research Center has studied a number of antenna structures for use as LSS; among which are the box truss (BT), tetrahedral truss (TT), radial rib, hoop column, and box ring truss. The study presented in this paper is similar and uses the computer-aided design system described in reference 1. The STAS is configured not as a complete antenna with reflector dish and feed mast, but as a parabolic planar (dish only) BT or TT structure. This experiment configuration provides information on both truss structures and antenna designs (deployment of curved surfaces, mesh management, and shape accuracies) as well as complementary information for linear structure experiments such as beam dynamics and SADE. In addition, the BT and TT structures were selected because they compare favorably with the hoop-column and radial-rib antenna concepts (ref. 2) and are more adaptable to other LSS uses such as solar array panels, support structures, and service facilities. They can be designed for complete deployment or be used to erect larger structures from smaller deployable modules.

The STAS consists of four antenna dishes packaged and mounted to the STEP as shown conceptually in figure 1. The deployed configurations are shown in figures 2 and 3. The larger dimension of the antenna, referred to as the diameter, corresponds to the antenna aperture that can be accommodated by mounting an

RF reflecting mesh to the structure. The antenna dish structures are maneuvered by the Shuttle remote manipulator system (RMS), which connects to each through the payload-mounted grapple fixture.

The STAS is instrumented with accelerometers, strain gauges, thermistors, surface measurement hardware, attitude sensors, a structural excitor, a telemetry transmitter and antenna, a transponder, and an attitude control system. The experiment begins with the RMS attaching to the folded antenna on the STEP. The RMS then places each STAS into a free-flying environment where deployment and structural measurement will occur. (Langley studies of similar configurations show that at an altitude of 400 km (the altitude used in this study), the separation distance between the Shuttle and the antenna is about 1 m in the first 4 min and 7 m after 10 min.) The STAS then is retrieved and attached to a STEP-mounted fixture where temperature and surface accuracy measurements and a structural modal survey are made. In the final phase, the STAS is again placed in a free-flying orbit where the measurement of temperatures, drag characteristics, and possibly structural characteristics is made. During this limited-lifetime orbit, data are transmitted periodically and the STAS is tracked for orbital characteristics. Orbit lifetime is estimated to be 10 to 20 days. The STAS will be destroyed during entry.

Although the major thrust of this paper is the flight experiment with a description of the antenna hardware, equally important to this development and design certification project is an extensive program in both ground testing and analyses. It is important that each of these areas be correlated with the other two. Development, engineering, and flight assurance ground testing need to be correlated both with analyses and the flight hardware activities; developments and improvements in analytical techniques, including new and improved computer programs, need to be correlated with testing and flight hardware, especially with respect to problems related to size and environmental differences (i.e., scaling, $1g$ versus $0g$, and damping). Although no RF or LSS controls hardware and testing are proposed for the flight test, these items may be included in ground testing and related to flight data. It is intended that the cost of the STASEP be kept to a moderate level, whereas each phase of the ground testing and analysis, which can be done incrementally, provides useful information for LSS design, irrespective of an ultimate flight test.

Conceptual Design of Scaled Truss Antenna Structures

Basic Structural Properties

Euler loading. Important to the design of truss-type LSS is the load-carrying capacity of the long slender structural members, which is limited by the critical stress in Euler buckling. For a thin-walled cylindrical column (assuming that $D_o^2 + D_i^2 = 2D^2$), the critical stress is proportional to the modulus of elasticity E divided by the square of the ratio of length to diameter (slenderness ratio) of the column. A plot of $\frac{\sigma_{cr}}{E} = \frac{\pi^2}{8(L/D)^2}$ is shown in figure 4, showing the inverse-square relationship of critical stress to slenderness ratio for a column pinned at both ends. Indicated in the figure are member L/D ratios of the 15-m STAS, a four-bay 45-m BT, a four-bay 45-m TT, and the EOS BT (study) antenna with 15-m-long elements. The ratios L/D for studies of this type are generally from 100 to 200. To help comprehend the sizing of tube members for these types of structures, information is given in figure 5 showing a family of curves relating column loading to the required tube diameter and tube length. A constant value (150 GPa (21.8×10^6 psi)) of longitudinal modulus of elasticity, representative of graphite/epoxy composite materials, has been used throughout this study. Rather than be limited to a set of load curves with a given tube wall thickness, each curve in the family has a value which is the ratio of the column load in Newtons to the wall thickness of the tube in millimeters. For example, on the curve for $P/t = 1000$, the circled point defines a tube of 5 cm diameter and 8.5 m length, which can carry a load of 1000 N with a wall thickness of 1 mm or 500 N with a wall thickness of 0.5 mm. As a point of reference, dashed lines for L/D are included. In summary, this figure parametrically relates the variables of Euler column buckling: column load, tube length, tube diameter, and tube wall thickness.

Member sizing. An important part of the STASEP is the concept of scaling (discussed in greater detail in the section entitled "Preflight Analysis"). When large structures are scaled down, serious problems can occur because of material and manufacturing limitations. This is especially important with regard to tolerances and thin-gauge material sections. In addition, joint and hinge characteristics are among the least understood inputs in characterizing LSS, and the problem is further exacerbated by having to deal with scaling to a number of different sizes and tolerances, which in some instances may not be practical or even possible. It was decided, therefore, to use a tube of the same diameter D and wall thickness t for all models studied. A wall thickness of 0.75 mm was chosen, since it represented a value with a margin above the typical minimal thickness for graphite/epoxy (about 0.5 mm). The greater thickness also helps in increasing the load-carrying capability of the member when faced with scaling to larger structures. Past studies indicate that a design load of 1000 N is both reasonable and conservative; this gives a value of P/t of 1333. Referring again to figure 5, the

circle at the intersection of the curve for $P/t = 1333$ and the dashed line at a diameter of 5 cm indicates the design point. This design point calls for a tube length of 7.5 m for the design case of $P = 1000$ N, $t = 0.75$ mm, and $D = 5$ cm. Moving to the left on the dashed line (at a diameter of 5 cm) results in increasing values of P/t and, therefore, larger loads are allowable (t is constant). The range of lengths of members in the 6- and 15-m STAS, represented by solid bars, shows that these structures are overdesigned with respect to Euler buckling. Where the curve for $P/t = 1333$ corresponds to these lengths, design-load diameters would be about 2 cm and 3 cm, respectively. Moving to the right on the dashed line (5 cm tube diameter), it intersects the curve for $P/t = 500$ at a point approximately midway on the bar representing the lengths of members in the 45-m scaled-up STAS. Using $t = 0.75$ mm, allows a load in the neighborhood of $P = (0.75)(500) = 375$ N for these structures. Studies of various LSS antenna concepts have shown member loads in the range of 400 N to 1000 N, depending on design and material properties. In summary, it is reasonable to conclude that the chosen tube dimensions ($D = 5$ cm, $t = 0.75$ mm) represent a reasonable center position for LSS member design. For example, a 10-m length ($L/D = 200$) corresponds to an allowable Euler load of 545 N.

Material properties. Other reports (for example, ref. 3) have discussed the merits of using laminated graphite/epoxy (Gr/E) materials for proposed LSS applications. The objectives of this experiment can best be satisfied by using Gr/E, and it was, therefore, chosen for this study. Values of Gr/E properties are given in table 1, as well as section properties of the cylindrical thin-walled tube used for the basic member.

Structural Definition

Basic structure. Both the TT and the BT structures are based upon modular, collapsible elements used as building blocks to form a large repetitive structure. The elements, shown in figures 6 and 7, are designed and assembled to form LSS in such a way as to allow them to be folded together compactly for stowage and launch. The shape (flat or curved) of the BT is controlled by the length of the diagonals in the face of each box. A flat structure will have boxes with rectangular faces, while a curved structure will have boxes with nonrectangular faces in the shape of a parallelogram. The shape of the TT is determined in a similar manner—appropriate lengths of the members of the tetrahedral modules. For this study the curvature of the structures was that of a paraboloid (only the connecting nodes fall on the parabolic surface), with a ratio of focal length to diameter of 1.5. The design included weights for connectors (spider joints, end fittings, hinges, and joints), RF mesh, and standoffs (the hardware mesh surface will be parabolically shaped by tying it to the standoffs and the structure). In this structural definition study, no weights were included for wires, cables, deployment mechanisms, instrumentation previously mentioned (accelerometers and telemetry), or a grapple fixture. Based on past studies, a rough estimate of this weight would be about 50 percent of the structure weight. These studies were made by using only the basic structural weights, since the basic concepts are more easily envisioned and the comparisons and performance estimates involve fewer assumptions and are more basic and straightforward.

Stowage and mass properties. When the BT is folded, the top and bottom horizontal (surface) elements hinge at their midpoints and are nest-folded double between the vertical members. Since allowance must be made for end fittings and mesh, the stowed length will be about 10 percent longer than the length of a vertical member, or 1.1 times the diameter of the antenna divided by the number of bays (four in this design). With the TT, the surface members also hinge in the middle and nest against the interior diagonals. In this study, these diagonals are longer than one-half the surface members, so that the stowed length is the sum of the diagonal length plus allowance for the depth of the parabola, the end fittings, and the mesh. The stowed crosswise dimensions of the STAS will vary little as a function of deployed diameter, since the member diameters are the same. The stowed crosswise dimension (diameter) of the TT is 1.63 m; the stowed crosswise dimension (the length of the side of a square) of the BT is about 0.8 m. The stowed dimensions of 6-, 15-, 30-, and 45-m-diameter antennas, the larger two given for comparison of the scaled-up versions with the smaller ones, are given in table 2.

The conceptual design of the STEP shows a platform 2.7 m wide and 2.9 m long. It has a freon pump attached to one end, adding another 0.3 m to the required length in the longitudinal dimension for a total of 3.2 m. The stowed lengths of the 15-m STAS are both longer than 3.2 m; thus, added length and provisions for mounting an overhanging package on the STEP are required.

The mass properties of the 6-m and 15-m TT and BT STAS are given in table 3 with those of the 30- and 45-m STAS given for comparison.

STAS Analyses

Thermal analysis. The transient thermal response is calculated over a designated portion of an orbit of each structural member, and its temperature is given

for the final position in the orbit. The temperature history of each member is calculated from the thermal radiation heat balance resulting from solar, Earth albedo, and Earth thermal radiation and the reradiation of thermal energy to space and toward the Earth. Each member is considered to be isothermal with no radiation, conduction, or shadowing among members; shadowing of members by the RF mesh (for the TT only) and Earth is included. A more detailed discussion of the IDEAS thermal capabilities is given in reference 1. This reference also concludes that worst-case conditions for distortion and thermal loading of the structure occur with edge-on solar heating. Although cases were computed for a noon orbit where $\beta = 90°$, the studies herein concentrated on the $\beta = 0°$ (or near zero) cases with edge-on heating, since $\beta = 90°$ cases had thermal loadings that were less severe. Because of the nature of the structure and to some degree the assumptions used in the analysis, maximum thermal structural loads occur in sunlight, with some combination of maximum and minimum member heating, and not during transit in or out of sunlight.

The sensitivity of the TT STAS to thermal loading in edge-on heating was investigated by varying the direction of the solar vector relative to the spacecraft, while holding the angle of the orbit ascending node, Ω at 90°.

First, the spacecraft was flown one complete orbit with an inclination i of 90° at different yaw angles. This configuration results in the Z-axis always pointing in the nadir direction, with the solar vector in the X-Y plane at a constant yaw angle ψ, as shown in figure 8. The loading of members 1 and 2 of the TT (fig. 9) increases sharply as ψ approaches 30° and is caused by temperature changes due to solar orientation and shading from the RF mesh. The temperature of members 1 and 2 dropped to around 200 K, whereas that of nearby members was around 300 K, and the loading doubled from 115 N for the nominal case ($\beta = 0°, \psi = 0°$) to 235 N for $\psi = 27.5°$. The above calculations were made with nominal values of mesh transmissivity, 0.9 (no mesh is 1.0), and mesh standoff distance, 0.375 m (about 30 percent of the STAS thickness). A case run with a mesh standoff distance of about 10 percent of the STAS thickness brought the mesh closer to the structure and thus internal members were shaded that had before been free of mesh shading. For the nominal case ($\psi = 0°$), the highest load was in member 12; its temperature decreased about 125 K and the load increased from about 110 N to 360 N. If this load were doubled as in the case of $\beta = 0°, \psi = 27.5°$ because of increased yaw, the maximum loads would become about 75 percent of the 1000-N design load and would represent a worst case. The smaller mesh standoff would not be used in the flight design, but the STAS could, however, orient itself unfavorably if it does not have attitude control. For an operational spacecraft, the $\psi = 27.5°$ case should not occur, but it would be desirable to design to survive such an anomaly.

Second, the spacecraft was flown in an operational orientation with the X-axis in the direction of flight and the Z-axis pointing to nadir. The orbit inclination angle was varied near $i = 90°$, with selected member loading occurring as in figure 10. (Note that the nominal case of $\psi = 0°$ in fig. 9 with member 1 at 115 N is the same as the case of $i = 90°$ in fig. 10.) In this operational case, the maximum loads are about 140 N at $i = 88°$. The heating rates for those members in figure 10 are given in figure 11, and the changes due to mesh shadowing are shown. A histogram of loading for the TT front members (mesh side) for the nominal case is given in figure 12.

In summary, thermal loading of TT members is higher for conditions of edge-on heating where mesh shading occurs and is sensitive to relatively small changes in solar orientation. Care must be exercised with antenna design concerning mesh placement and, possibly, limiting operational orientations to stay within lower design loads that would allow for lower spacecraft weight.

Similar studies were made for the BT STAS with regard to the change of ψ, but shading by the mesh was not included because it had not been included in the computer program. These results (at the end of one-half orbit) are given in table 4. Maximum loads occur at an orientation of $\psi = 0°$, where one-half of the horizontal surface members are perpendicular to the solar vector and the other half are parallel to it, because of maximum and minimum expansion and contraction of these members. In all cases, the vertical members are perpendicular to the solar vector and experience maximum heating. There was no pretensioning of the diagonal members—as would be true for an operational design—but their loads were never excessive, being 44 N and −14 N for the $\psi = 0°$ case and 9 N and −60 N for the $\psi = 45°$ case. This low loading allows for pretension in the cord-like retractable diagonals. The extreme compressive loading occurred in the top surface members (bottom members follow the same pattern) as shown in table 5.

For comparison between the BT and TT in the operational mode, two nominal cases ($i = 90°, \psi = 0°$) were run: (1) a TT with no mesh giving a minimum load of −1 N (compared with the BT at −85 N) and (2) a BT with the temperatures of two mesh side members set at 200 K to simulate shading giving a minimum load of −205 N (compared with the TT at −114 N).

Structural loading. Early studies included gravity gradient and aerodynamic loads, but with values of less

than 0.1 N, they were subsequently neglected. Loads from in-orbit control were also neglected since orbit changes and antenna slewing will not be performed, and attitude control, if included, will utilize low-level thrusters. No attempt was made to analyze in-orbit or ground handling loads. The peak response acceleration load from random vibration during the Shuttle launch was roughly estimated based on the natural frequency response of a simply supported tube representing the longest STAS member. This tube has the following characteristics:

$D = 5$ cm

$t = 0.75$ mm

$L = 3.75$ m

$y = 0.9$ mm ($1g$ deflection due to its own weight)

$f_n = 18.9$ Hz

A natural frequency of 20 Hz was used in the following formula:

$$G_R = C\left[\frac{\pi}{2} Q_R f_n \mathrm{ASD}\right]^{1/2}$$

A value of ASD of 0.0007 g^2/Hz was used and represents the expected response from the Shuttle main longeron trunnion fitting at 20 Hz (ref. 4); then,

$$G_R = 2.2\left[\frac{\pi}{2}(10)(20)(0.0007)\right]^{1/2} = 1.0g$$

Shuttle launch loads in the direction of the Z-axis (normal to the tubes) are $2.5g$ or less; the emergency landing load factor is $4.5g$. At $1g$, the stress in the tube with $D = 5$ cm, $t = 0.75$ mm, and $L = 3.75$ m, from its own weight normal to its axis, is 2.25 MPa; at $2.5g$, it is 5.62 MPa; and at $4.5g$, it is 10.12 MPa. Comparing these stresses with an ultimate strength of 0.15 GPa (an ultimate strain of 0.001), the worst case is lower by an order of magnitude. The Shuttle launch loads should not be a problem; this, of course, depends upon the design of the packaged configuration.

Most calculations of thermal loads in this study used $\alpha = -4 \times 10^{-7}$ K^{-1}. This represents a graphite/epoxy (Gr/E) material with unidirectional laminates in the longitudinal direction, as shown in figure 13. Higher values of α result in linearly proportionally higher values of thermal loading and, in addition, lower values of the modulus of elasticity E (stiffness). To move toward a Gr/E with a higher α and lower E would quickly result in large penalties in weight, package volume, and thermal distortions. For example, figure 14 shows the weight penalty (about 30 percent) for a 45-m-diameter antenna when the column load is increased from 300 N to 1000 N and the tube diameter must be increased from 5.0 cm to 7.5 cm. These facts should eliminate considerations of using aluminum for these flight models and studies. Its α is more than 50 times higher than that used in this study and its stiffness less than half; thus, the P/E term in the Euler column formula (fig. 5) is more than 100 greater than that of Gr/E. In addition, the use of a material in scaled flight experiments different from what will be used for flight hardware will complicate the dimensional analysis and scaling laws that are an important objective of the STASEP.

In summary, the STAS is adequately designed to meet the thermal and structural loading requirements of this experiment.

Structural dynamics. The natural frequencies of the BT and TT 6-m and 15-m STAS and of scaled-up models with 30-m and 45-m diameters were determined for both free and clamped boundary conditions and are given in table 6 for the first six nonrigid body modes. Mode shapes are shown in figures 15 through 18 for the 15-m BT and TT. These frequencies and mode shapes were calculated by using the General Dynamics SOLID SAP computer program, a finite-element structural analysis program for the dynamic linear elastic analysis of three-dimensional structural systems. The mode shapes were generated by using the interactive plotting module and data from the SAP dynamic solutions. The original structure is shown by dashed lines with the displaced shape (exaggerated) shown by solid lines. The maximum normalized displacements—dx, dy, and dz—are given. For clarity, only the dish surface structural members are given for the TT.

In the clamped cases, the structure was restrained (no rotations or displacements) at two points. For the TT, one point was between members 1 and 9 (mesh side), and the other was at the apex (back side) of the tetrahedron whose base is formed with member 12 and contains the first point. For the BT, the two points were both at one corner, one on the front and the other on the back of the structure.

Preflight Analysis

The preflight or ground analysis and testing phases, along with the flight phase, complete the triad of activities necessary for a complete and successful STASEP. A portion of these activities is basically an extension of the standard approach presently used for dynamic modeling and analysis accompanied by a corresponding test program. There are, however, major differences because of the inability to test large full-scale models and to duplicate the $0g$ environment. In addition, factors such as nonlinearities, unknown damping characteristics, joint and hinge hysteresis, and a high number of degrees of freedom (many structural members) combine to present a difficult challenge for analytical modeling

and its correlation with test and flight data. This challenge requires an extension of existing techniques as well as the development of new techniques; larger and more complicated computer programs (more complex structures); effective reduction of model complexity, scaling, modal surveys, simulation of on-orbit deployment and dynamics; and good design information for control systems.

Scaling automatically becomes a consideration in the analysis and testing of the STAS's, since they represent subscale models of potential operational LSS. There are two means of predicting the structural and dynamic characteristics of a proposed physical system. The first is through the use of a mathematical model and analysis. The second is through tests on a prototype, or properly scaled and understood model, with considerations for the test environment. The STASEP will use both means to verify the predictions of and the correlations between the mathematical and physical models, to account for the differences between the ground and flight environments, and to provide the basis for predicting the behavior of full-size LSS. A practical difficulty with scaling is that it is impossible to satisfy all the requirements for similitude that are theoretically necessary; the only scale factor compatible with all requirements is unity (identical geometry, size, and materials). This is a special case of replica scaling, which is defined as identical geometric scaling with prototype materials. Similitude requires that the nondimensional quantities representing the model and prototype characteristics be the same for both the scale model and prototype. For example, consider a nondimensional scaling parameter (NSP or Π_1) representing the ratio of inertia forces to elastic forces:

$$\Pi_1 = \frac{\rho\omega^2 L^6}{EI}$$

The replica scaling ratios (identical materials) are then $E_m = E_p, \rho_m = \rho_p$. Equating the NSP for the model and prototype gives

$$\Pi_{1,m} = \Pi_{1,p}$$

$$\frac{\omega_m^2 L_m^6}{I_m} = \frac{\omega_p^2 L_p^6}{I_p}$$

and since for geometric scaling $I = f(L^4)$, the ratio

$$\left(\frac{L^4}{I}\right)_m = \left(\frac{L^4}{I}\right)_p$$

then

$$\omega_m^2 L_m^2 = \omega_p^2 L_p^2$$

or

$$\omega_m L_m = \omega_p L_p$$

In this case, where the product ωL is the same for both model and prototype (referred to as constant-velocity models), corresponding scaled amplitudes will have the same vibration velocities and the same stresses caused by vibration.

Consider further the NSP(Π_2) for the ratio of vibration acceleration to gravity acceleration

$$\Pi_2 = \frac{\omega^2 L}{g} = \frac{(\omega L)^2}{Lg}$$

Models scaled to satisfy this NSP(Π_2) will simulate phenomena such as static deflections, landing dynamics and stability, and the ratio of fuel slosh frequencies to vibratory frequencies. Using the previous case of replica scaling with identical materials where $\omega_m L_m = \omega_p L_p$, and equating give

$$\Pi_{2,m} = \Pi_{2,p}$$

then

$$L_m g_m = L_p g_p$$

Thus, if vibrational stresses, static stresses, and dynamics are to be simulated, the model must be tested in an acceleration field where Lg is the same for model and prototype. An example of this approach was demonstrated with the lunar landing vehicles where 1/6-scale models (the ratio of the gravity fields of the Moon and Earth) were tested on Earth. Although it is logically or even intuitively obvious that a $0g$ environment cannot be directly simulated on Earth, the above equation shows mathematically that it is impossible since the scale model would require a length of zero. Thus, a model of a prototype structure that would operate in orbit in the $0g$ environment with no static stresses (or deflections) will always have some static stresses proportional to its size that will affect deployment, shape, and stress levels when tested on Earth.

It is usually not practical to build a replica model (identical geometric scaling and details with the same materials as in the prototype) because of practical considerations such as the cost of duplicating structural detail (including joints and hinges), the fabrication difficulties of working with scaled-down sizes and tolerances, and the advantages of meeting objectives with a less complicated and costly model. In these instances, either direct similar geometric scaling or general distorted scaling can be used. Direct similar geometric scaling is nearly the same as replica scaling but exact detail is not always simulated. The overall geometry, mass, and stiffness properties of the prototype are directly simulated but the model is only similar and may use different materials and have moderate deviations from properly scaled dimensions. This method

can result in substantial savings in design and fabrication costs and time with little loss of accuracy. General distorted scaling can be used when replica and direct geometric scaling is not required (limited simulation) or possible. Distorted scaling may use different materials, or the length scale factor may not be maintained throughout the structure. Some NSP's, therefore, are not correct and model properties must be expressed in such a way as to compensate for these distortions and allow for understanding the modeling laws that mathematically relate the characteristics between the prototype and model systems for the phenomenon being investigated.

The scaling down of a large STAS of 45 m to 6 m would result in a very thin wall thickness (0.1 mm), small diameters (0.67 cm), and extremely small tolerances (0.0034 mm) for a precision fit. These small dimensions and tolerances would be impractical, if not impossible, in terms of their effect on fabrication, cost, and quality assurance, especially with regard to the high part count and complexity related to the STAS type of structure. In addition, the strength of the 6-m structure would not be adequate for assembly and testing (such as deployment and surface accuracy) in the $1g$ Earth environment. It was decided, therefore, to use the general distorted scaling approach for the STAS and to require that the member tube diameters and wall thickness be the same for all structures. There are other advantages to this approach, mainly by avoiding complications in the areas of fabrication, characterization, and modeling uncertainties of items such as joints, hinges, and actuation systems (for deployment), which have a large effect on these structures. The added dimension of understanding the relationships among a number of different sizes (diameters) of these items could be formidable, since they are likely not to be linear and to be complicated by fabrication and assembly variations. A great deal of effort will be required to design optimum systems of these types for just one size, considering the large number of unknowns and variables such as (1) the effects of joint/hinge friction, hysteresis, and damping on dynamic response; (2) how to design a joint/hinge that can be understood, characterized, and accurately modeled for analysis; (3) how to relate design, precision, and tolerances to characterization, reliability, quality assurance, modeling uncertainties, dimensional stability, and assembly variations; and (4) how to relate the variable nature of the large number of manufactured component piece parts and subassemblies to the reliability, flight qualification, flight assurance, characterization, and analysis performance of the assembled structure.

As an illustration, and to provide an approximate relationship of the scaling involved with STASEP, the NSP relating frequency of vibration and size is derived. The first bending frequency of vibration for a free-free isotropic square plate is (ref. 5)

$$f_p = \frac{14.1}{2\pi L^2}\sqrt{\frac{S}{\rho t}}$$

This equation, with certain assumptions and derivations, may be written for an equilateral tetrahedral truss with square planform as

$$f_t = \frac{14.1}{4\pi\sqrt{6}}\frac{\ell}{L^2}\sqrt{\frac{E_c}{\rho_c}}$$

The dimension ℓ for a four-bay structure can be expressed in terms of L as

$$\ell = \frac{L}{4\sin 60^\circ} = \frac{L}{2\sqrt{3}}$$

Then

$$f_t = \frac{14.1}{24\pi\sqrt{2}}\frac{1}{L}\sqrt{\frac{E_c}{\rho_c}}$$

Expressing this as the nondimensional scaling parameter

$$\Pi_3 = \frac{14.1}{24\pi\sqrt{2}}\frac{1}{fL}\sqrt{\frac{E_c}{\rho_c}}$$

and setting $\Pi_{3,m} = \Pi_{3,p}$ when $E_{c,m} = E_{c,p}$ and $\rho_{c,m} = \rho_{c,p}$,

$$\frac{1}{f_m L_m} = \frac{1}{f_p L_p}$$

or

$$f_m L_m = f_p L_p$$

This equation illustrates for the simplified case just described that the frequency times the length of a side is a constant for all models. This was found to be generally true for the STAS structures studied (the nonlinear effects of mesh weight and end fittings cause deviations from fL = Constant). For example, the product fL for the first modes of the 6-, 15-, 30-, and 45-m tetrahedral truss structures are 345, 375, 372, and 360, respectively. Similarly, for the box truss, they are 410, 445, 464, and 468.

The modeling of LSS presents a problem that is perhaps more difficult than others, since the degree of similitude required in the scale-model test increases as the capability of the analytical modeling decreases. Mature analytical techniques for modeling LSS does not yet exist and actual fabrication of accurate LSS models will be difficult. This is a new area of modeling where experience is needed; the application of techniques to actual physical problems is partially an art as well as a science, and it strongly depends on insight, knowledge, and experience in the field. Virtually every simulation

effort will have some parameters that are not satisfied or are approximated in the physical modeling. The goal, therefore, since complete simulation is not possible, is to design and develop hardware, testing, and analytics that are practical and meet the specific needs of the problems being studied.

In summary, the objectives of the analysis and software effort are to develop new and more advanced analytical techniques and computer programs for structural characterization; an analytical understanding of scaling, and its correlation with ground test, simulation, and flight experiment data; techniques for handling, reduction, and use of ground test and flight test data.

Preflight Testing

The testing phase of the STASEP will support hardware development, analytical techniques, and structural characterization and provide for qualification and flight assurance testing. No attempt has been made here to detail a comprehensive test program. Items that need to be considered in testing have been separated into two areas: (1) development testing and (2) qualification and flight assurance testing, and they are presented in outline form as follows:

Development testing

- Components
  - Scaled hardware development
  - Joint and hinge development
  - Releasing and deployment mechanisms
  - Material selection and characterization
  - Sensors and instrumentation
  - Test and support equipment
- Scale models and full-scale partial models
  - Structural characterization
  - Mesh integration and management
  - Deployment of mesh and structure
  - Mesh shaping and surface measurement
  - Thermal simulation
  - $0g$ simulation
  - Kinematic performance
  - Component mounting
  - Cable routing
  - Structural shape and distortion effects
- Analyses and software
  - Determine scaling effects
  - Structural characterization
  - Deployment mechanics (computer model)
  - Mesh shaping and adjusting techniques
  - Measurement of surface accuracy
  - Shape and distortion predictions
  - $0g$ versus $1g$ compensations
  - Thermal performance
  - Data handling and reduction
  - New computer programs
  - Verification and analytical predictions

Qualification and flight assurance testing

- Design verification (qualification testing)
- System compatibility and checkout
- Analysis and test data correlation
- Flight readiness (flight assurance testing)
- STEP interface verification
- STS safety
- STS interface verification

Concluding Remarks

A scaled truss antenna structures experiment program (STASEP) has been initially defined with the objective of advancing the knowledge and confidence level for producing flight-qualified hardware for large space systems (LSS). Specific overall objectives are

1. To understand and predict the physical characteristics of large space structures
2. To develop $1g$ approaches for ground testing and qualifying LSS which will be deployed and operated in the $0g$ environment
3. To advance the technique of using scale models and full-scale partial models in analyzing and testing LSS
4. To develop operational techniques for the handling and testing of large lightweight structures
5. To gain experience, through the use of subscale pathfinder mode s, in the testing, integration, and launch and orbit operations of LSS
6. To employ and advance space environment testing and experimentation utilizing the Space Technology Experiments Platform (STEP) as a test facility

The STASEP uses four scaled truss antenna structures (STAS) in a design, development, testing, and flight experiment program designed to relate analyses, simulation, scaling, ground testing, and actual in-orbit performance. Two types of STAS, tetrahedral truss (TT) and box truss (BT), and two sizes, 6 m and 15 m, are to be mounted to the STEP and carried into orbit by the Shuttle. The STAS will be serviced by the STEP and Shuttle remote manipulator system (RMS) in an experiment sequence that provides data on deployment, structural characteristics, geometric accuracies, and thermal performance. A final phase of the experiment, with the STAS in a free-flying mode, will provide additional data, including aerodynamic drag, until reentry.

The STAS will be constructed from graphite/epoxy tubes, 5 cm in diameter with a 0.75-mm wall thickness, and connected by hinges and end fittings. The basic structural weight (including connectors, hinges, and radio-frequency (RF) mesh but no instrumentation or deployment hardware) of the 15-m TT is 96 kg (211 lb); the 15-m BT is 135 kg (297 lb). The study shows that the 6- and 15-m STAS are capable of meeting all structural loading requirements of the experiment. The study includes a discussion of analyses (including scaling) and testing.

Data from the 6- and 15-m flight model experiment will be used to develop scaling laws for application to 30- and 45-m antenna dish designs and other generic LSS. With the STASEP philosophy it is envisioned that larger scaled-up structures will require only modest changes in structural materials, mechanism design (including size), and member sizing. Truss member lengths can be limited by increasing the number of bays; thus, the problem of dealing with Euler buckling is alleviated.

As defined, the STASEP is the first low-risk, low-cost LSS flight experiment proposed to provide technology validation and scaled design information for application to operational-type concepts. An important feature is its flexibility of implementation. Information generated throughout the program will be widely applicable and useful to LSS and not necessarily limited to the STASEP. Early phases of design, analysis, development, and testing can begin without the need for a commitment to the flight experiment or its detailed technical requirements.

Langley Research Center
National Aeronautics and Space Administration
Hampton, VA 23665
August 23, 1984

References

1. Garrett, L. Bernard: *Interactive Design and Analysis of Future Large Spacecraft Concepts.* NASA TP-1937, 1981.
2. Garrett, L. Bernard; and Ferebee, Melvin J., Jr.: Comparative Analysis of Large Antenna Spacecraft Using the IDEAS System. *A Collection of Technical Papers, Part 1: Structures and Materials—AIAA/ASME/ASCE/ASH 24th Structures, Structural Dynamics and Materials Conference*, May 1983, pp. 19–28. (Available as AIAA-83-0798.)
3. Bush, Harold G.; Mikulas, Martin M., Jr.; and Heard, Walter L., Jr.: Some Design Considerations for Large Space Structures. *AIAA J.*, vol. 16, no. 4, Apr. 1978, pp. 352–359.
4. Shuttle Orbiter/Cargo Standard Interfaces. *Space Shuttle Program Level II Program Definition and Requirements—Space Shuttle System Payload Accommodations.* ICD 2-19001, JSC 07700, Volume XIV, Revision H, NASA Johnson Space Center, May 16, 1983.
5. Mikulas, Martin M., Jr.; Bush, Harold G.; and Card, Michael F.: *Structural Stiffness, Strength and Dynamic Characteristics of Large Tetrahedral Space Truss Structures.* NASA TM X-74001, 1977.

Bibliography

Space Shuttle Program Level II Program Definition and Requirements—Space Shuttle System Payload Accommodations. JSC 07700, Volume XIV, Revision H, NASA Johnson Space Center, May 16, 1983.

Abramson, H. Norman; and Nevill, Gale E., Jr.: Some Modern Developments in the Applications of Scale-Models in Dynamic Testing. *Use of Models and Scaling in Shock and Vibration*, Wilfred E. Baker, ed., American Soc. Mech. Eng., c.1963, pp. 1–15.

Berry, R. L.: Lessons Learned on the Manned Maneuvering Unit Modal Survey Using Single Point Random Excitation. AIAA-83-1022, May 1983.

Coyner, J. V., Jr.: Box Truss Development and Applications. *Large Space Antenna Systems Technology—1982*, E. Burton Lightner, compiler, NASA CP-2269, Part 1, 1983, pp. 527–543.

Coyner, J. V., Jr.: 15-Meter Deployable Aperture Microwave Radiometer. *Large Space Antenna Systems Technology—1982*, E. Burton Lightner, compiler, NASA CP-2269, Part 1, 1983, pp. 131–155.

Fager, John A.: Large Space Erectable Antenna Stiffness Requirements. *Technical Papers—Seventh AIAA Communications Satellite Systems Conference*, Apr. 1978, pp. 415–422. (Available as AIAA Paper 78-590.)

Fager, J. A.: Status of Deployable Geo-Truss Development. *Large Space Antenna Systems Technology—1982*, E. Burton Lightner, compiler, NASA CP-2269, Part 1, 1983, pp. 513–525.

Ferebee, Melvin J., Jr.; Garrett, L. Bernard; and Farmer, Jeffery T.: Interactive Systems Analysis of Four Structural Concepts for a Land Mobile Satellite System. AIAA-83-0219, Jan. 1983.

Farrell, C. E.; and Zimbelman, H. F.: *Advanced Space Systems Analysis Software—Technical, User, and Programmer Guide.* NASA CR-165798, 1981.

Garrett, L. Bernard: Thermal Modeling and Analysis of Structurally Complex Spacecraft Using the IDEAS System. AIAA-83-1459, June 1983.

Ibrahim, Samir R.; and Pappa, Richard S.: Large Modal Survey Testing Using the Ibrahim Time Domain (ITD) Identification Technique. AIAA-81-0528, Apr. 1981.

Jaszlics, I. J.; and Park, A. C.: *Use of Scale Models To Determine the Structural Dynamic Characteristics of Space Vehicles.* MCR-69-103 (Contract NAS8-21456), Martin Marietta Corp., May 1968. (Available as NASA CR-98479.)

Jaszlics, I. J.; and Park, A. C.: *Use of Dynamic Scale Models To Determine Launch Vehicle Characteristics—Final Report. Volume I. Analytical Investigation.* MCR-68-87 (Contract NAS8-21101), Martin Marietta Corp., Aug. 1969. (Available as NASA CR-102272.)

Keafer, Lloyd S., Jr.; and Hook, W. R.: A Summary of Mission and System Performance Requirements for Large Space Antennas. *Large Space Antenna Systems Technology—1982*, E. Burton Lightner, compiler, NASA CP-2269, Part 1, 1983, pp. 201–212.

Keafer, Lloyd S., Jr.; and Harrington, Richard F.: *Radiometer Requirements for Earth-Observation Systems Using Large Space Antennas.* NASA RP-1101, 1983.

Leondis, Alex: *Large Advanced Space Systems Computer-Aided Design and Analysis Program—Final Technical Report.* NASA CR-159191-1, 1980.

Leondis, Alex: *Large Advanced Space Systems Computer-Aided Design and Analysis Program—User Document.* NASA CR-159191-2, 1980.

Leondis, Alex: *Large Advanced Space Systems Computer-Aided Design and Analysis Program—Programmer Document.* NASA CR-159191-3, 1980.

Pappa, Richard S.: Some Statistical Performance Characteristics of the "ITD" Modal Identification Algorithm. *A Collection of Technical Papers, Part 2: Structural Dynamics and Engineering—AIAA/ASME/AHS 23rd Structures, Structural Dynamics and Materials Conference*, May 1982, pp. 622–640. (Available as AIAA-82-0768.)

Pappa, Richard S.; and Juang, Jer-Nan: Galileo Spacecraft Modal Identification Using an Eigensystem Realization Algorithm. *A Collection of Technical Papers, Part 2—AIAA/ASME/ASCE/AHS 25th Structures, Structural Dynamics & Materials Conference and AIAA Dynamics Specialists Conference*, May 1984, pp. 630–645. (Available as AIAA-84-1070.)

Penning, F. A.: *Use of Dynamic Scale Models To Determine Launch Vehicle Characteristics—Final Report. Volume II. Experimental Investigation.* MCR-68-87 (Contract NAS8-21101), Martin Marietta Corp., Aug. 1969. (Available as NASA CR-102280.)

Pinson, L. D.; and Amos, A. K.: NASA/USAF Research in Structural Dynamics. *Large Space Antenna Systems Technology—1982*, E. Burton Lightner, compiler, NASA CP-2269, Part 1, 1983, pp. 301–344.

Regier, Arthur A.: The Use of Scaled Dynamic Models in Several Aerospace Vehicle Studies. *Use of Models and Scaling in Shock and Vibration*, Wilfred E. Baker, ed., American Soc. Mech. Eng., c.1963, pp. 34–50.

TABLE 1. PROPERTIES OF GRAPHITE/EPOXY MATERIAL AND CYLINDRICAL THIN-WALLED TUBE

Property	SI Units	U.S. Units
E . . .	150 GPa	21.76×10^6 psi
α . . .	-4×10^{-7} K^{-1}	-2.22×10^{-7} °F^{-1}
ρ . . .	1633 kg/m^3	0.059 lb/in^3
a . . .	0.90	0.90
e . . .	0.80	0.80
c . . .	1.0 kJ/kg-K	0.239 Btu/lb-°F
D . . .	5.0 cm	1.968 in.
t . . .	0.75 mm	0.030 in.
A . . .	1.160 cm^2	0.180 in^2
I . . .	3.519 cm^4	0.085 in^4

TABLE 2. STAS STOWED DIMENSIONS

Antenna diameter, m	STAS stowed dimensions, m, for—			
	Box truss		Tetrahedral truss	
	Length	Crosswise dimension	Length	Crosswise dimension
6	1.65	0.80	1.42	1.63
15	4.12	.80	3.55	1.63
30	8.25	.80	7.10	1.63
45	12.37	.80	10.64	1.63

TABLE 3. GEOMETRY AND MASS PROPERTIES OF FOUR SIZES OF TETRAHEDRAL TRUSS AND BOX TRUSS STRUCTURES

Property	Tetrahedral truss STAS with diameter of—				Box truss STAS with diameter of—			
	6 m	15 m	30 m	45 m	6 m	15 m	30 m	45 m
Weight:								
Total, kg	45.0	96.0	190.0	295.0	63.0	135.0	270.0	450.0
Structure, kg	44.0	90.4	167.5	244.5	62.2	130.0	250.0	405.0
Mesh system, kg	1.0	5.6	22.5	50.5	0.8	5.0	20.0	45.0
Center of gravity$(-Z)$[a], m	0.20	0.47	0.87	1.26	0.50	1.25	2.36	3.40
Moment of inertia:								
I_{XX} and I_{YY}, kg-m^2	126	1654	13 270	47 300	293	3880	31 280	115 800
I_{ZZ}, kg-m^2	245	3222	25 870	92 280	513	6780	54 600	202 100
Average member length:								
Surface, m	1.75	4.44	8.89	13.33	1.50	3.75	7.50	11.25
Diagonal, m	1.14	2.87	5.77	8.64	[b]2.12	[b]5.30	[b]10.61	[b]15.91
Depth of structure, m	[c]0.51	[c]1.27	[c]2.55	[c]3.82	1.50	3.75	7.50	11.25

[a]Right-hand coordinate system with Z-axis coming out of center of concave surface of dish and pointing toward Earth ($Z = 0$ is at dish surface), X-axis points in direction of velocity vector.

[b]For operational design, box truss diagonal members are in tension (no Euler buckling).

[c]Depth determined by diagonal angle (see fig. 7); study used 30°.

TABLE 4. THERMAL LOADING OF BOX TRUSS STRUCTURE

[Zero stress condition is at 294 K (21°C)]

ψ, deg	α, K^{-1} (*a*)	Thermal loading, N, for—				Temperature range, K (*b*)
		Surface		Verticals		
		Min	Max	Min	Max	
0.00	-4×10^{-7}	−85	−22	−50	−13	208 to 316
	$+4 \times 10^{-7}$	34	100	22	60	
11.25	-4×10^{-7}	−44	−12	−28	−10	238 to 316
	$+4 \times 10^{-7}$	12	44	10	28	
22.50	-4×10^{-7}	−9	3	−15	−6	263 to 316
	$+4 \times 10^{-7}$	−3	9	6	15	
33.75	-4×10^{-7}	10	30	−14	−5	281 to 316
	$+4 \times 10^{-7}$	−30	−10	5	14	
45.00	-4×10^{-7}	18	68	−21	−4	212 to 316
	$+4 \times 10^{-7}$	−68	−18	4	21	

[a]Negative value indicates that material is contracting with increasing temperature, and plus value indicates that material is expanding.

[b]Temperature range of members but does not necessarily correspond to members with maximum and minimum loads.

TABLE 5. COMPRESSIVE LOADING OF SURFACE MEMBERS

ψ, deg	α, K^{-1}	Minimum load, P_{min}, N	Members experiencing P_{min}	Maximum load, P_{max}, N	Members experiencing P_{max}
0	-4×10^{-7}	-85 to -83	7, 8, 19, 27, 29, and 37	-26 to -22	5, 6, 17, 18, 25, 26, 35, and 36
45	$+4 \times 10^{-7}$	-68 to -65	1, 7, 13, 16, 21, 27, 34, and 39	-18	5, 6, 9, 12, 25, 26, 30, and 32

TABLE 6. NATURAL FREQUENCIES FOR FIRST SIX NONRIGID BODY MODES FOR STAS

Nonrigid body mode	Natural frequency, Hz, for STAS with boundary condition and diameter of—							
	Free				Clamped			
	6 m	15 m	30 m	45 m	6 m	15 m	30 m	45 m
Tetrahedral truss								
1	57.5	25.0	12.4	8.0	12.4	5.4	2.7	1.8
2	57.5	25.0	12.4	8.0	32.3	14.0	7.0	4.6
3	75.2	32.7	16.2	10.4	46.5	20.2	10.1	6.6
4	90.2	39.1	19.4	12.6	59.4	25.8	12.8	8.3
5	96.9	42.0	20.8	13.4	73.9	32.1	15.9	10.2
6	96.9	42.0	20.8	13.4	75.4	32.8	16.2	10.4
Box truss								
1	68.3	29.7	15.5	10.4	12.9	5.6	2.9	1.9
2	136.4	58.8	30.1	20.2	25.7	11.2	5.7	3.8
3	143.7	62.0	31.8	21.4	48.4	20.9	10.9	7.8
4	159.0	68.8	36.0	24.2	69.7	30.1	15.6	10.9
5	161.6	70.0	36.1	24.2	108.6	46.8	24.2	16.5
6	161.6	70.0	36.1	24.2	112.8	48.7	24.7	17.1

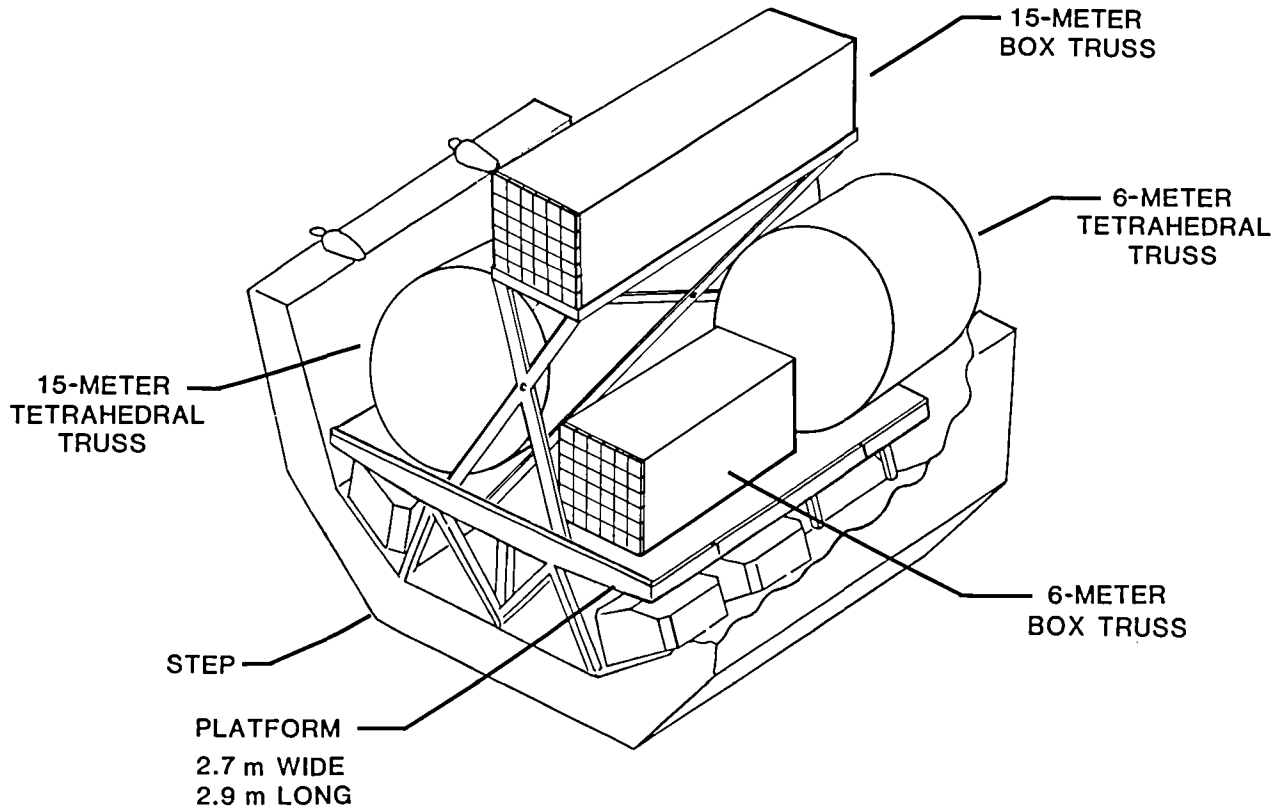

Figure 1. Launch configuration of STAS mounted to STEP.

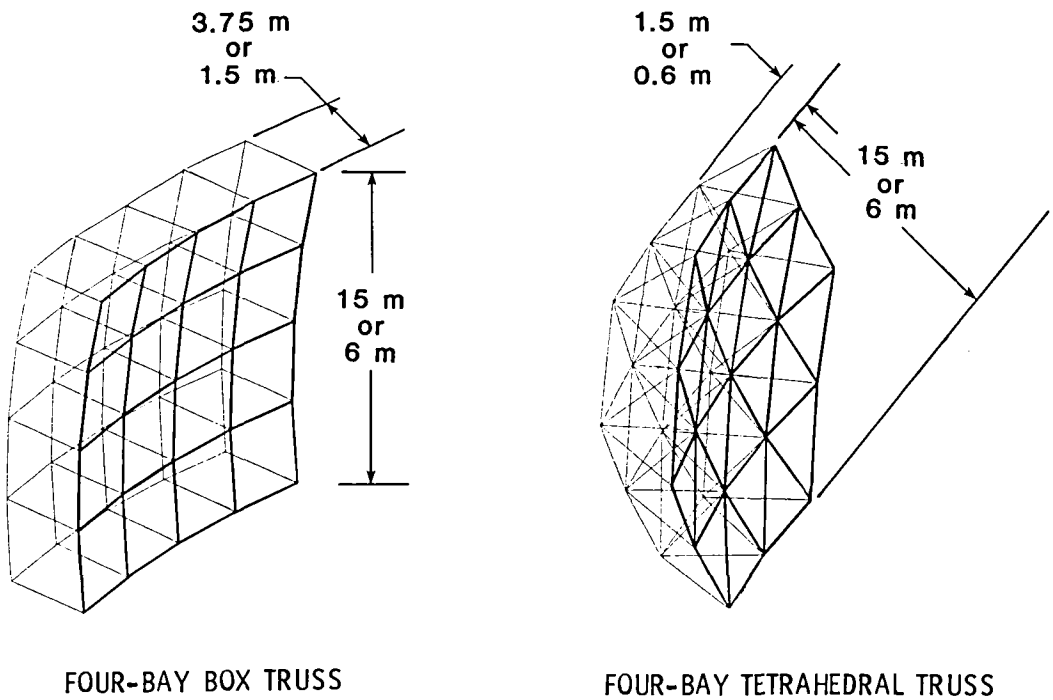

Figure 2. Box truss and tetrahedral truss configurations showing diameters and depths of four STAS's.

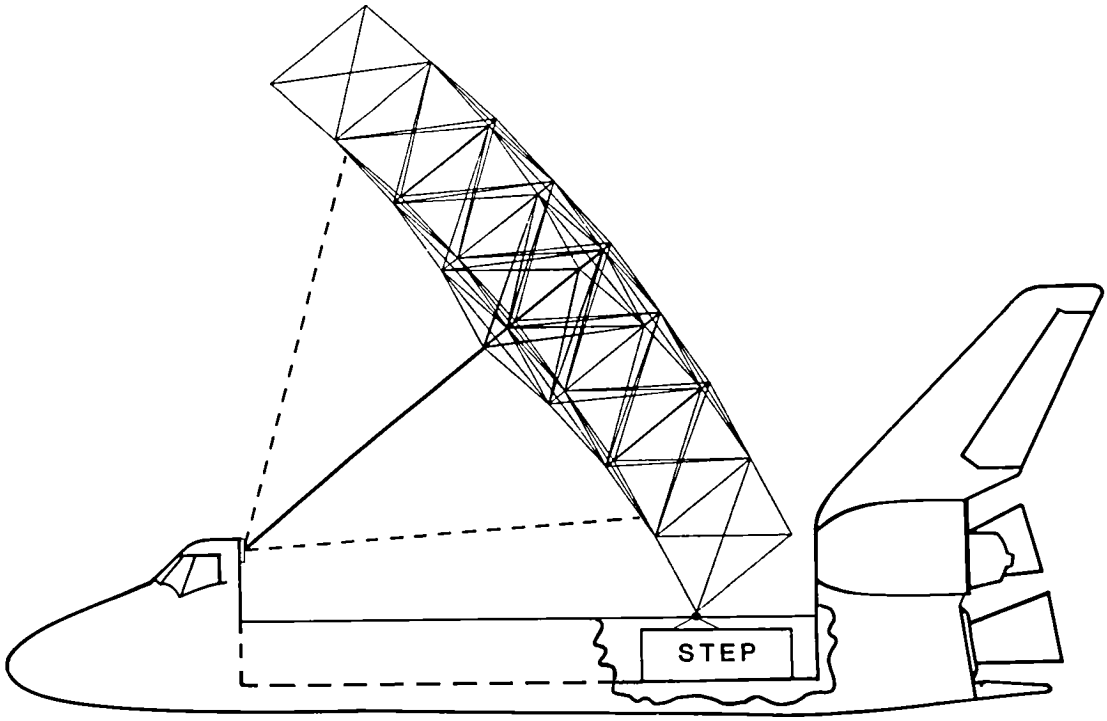

Figure 3. Shuttle/STEP-mounted 15-m box truss antenna.

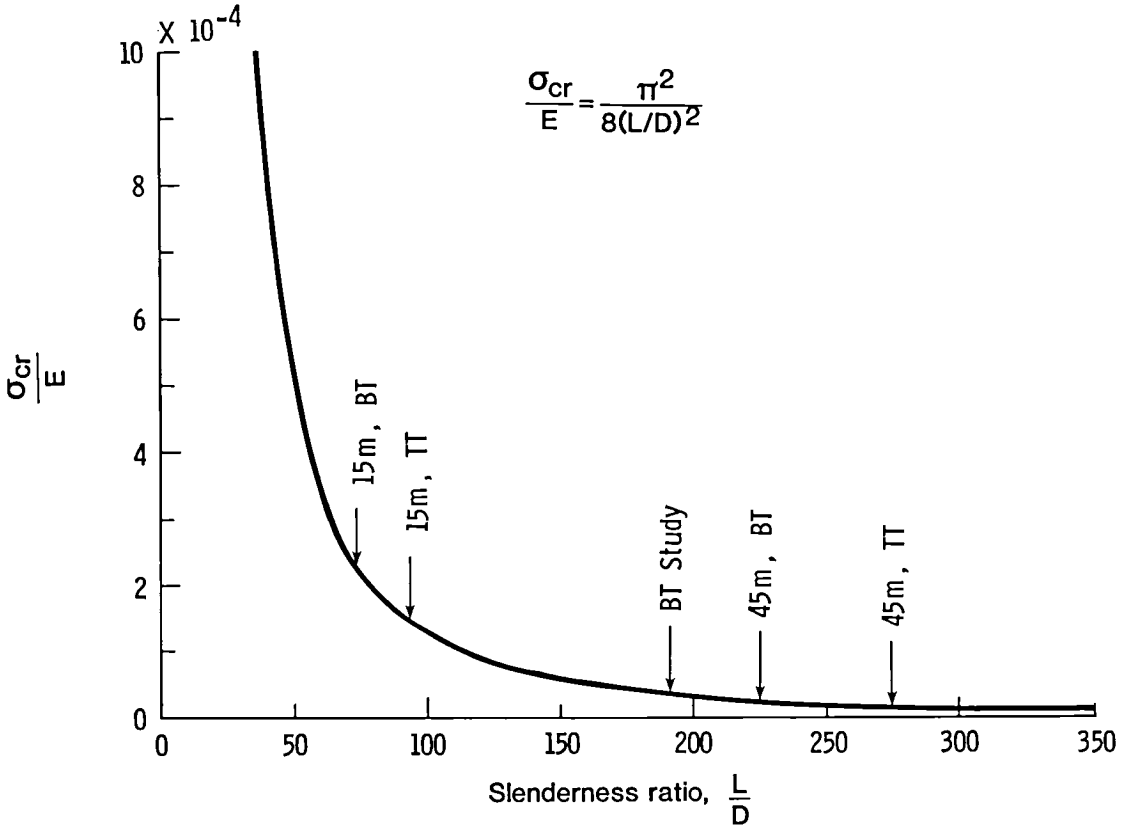

Figure 4. Effect of slenderness ratio on Euler critical stress for column pinned at both ends.

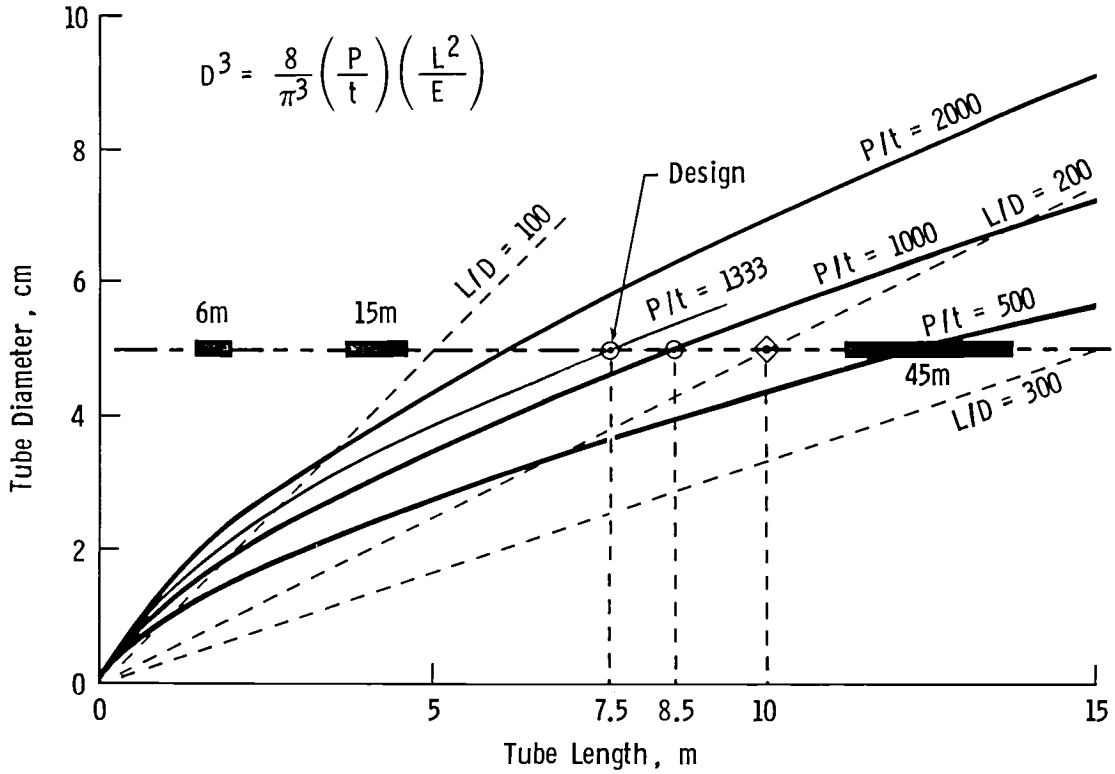

Figure 5. Relationship of Euler column loading to tube thickness, tube diameter, and tube length.

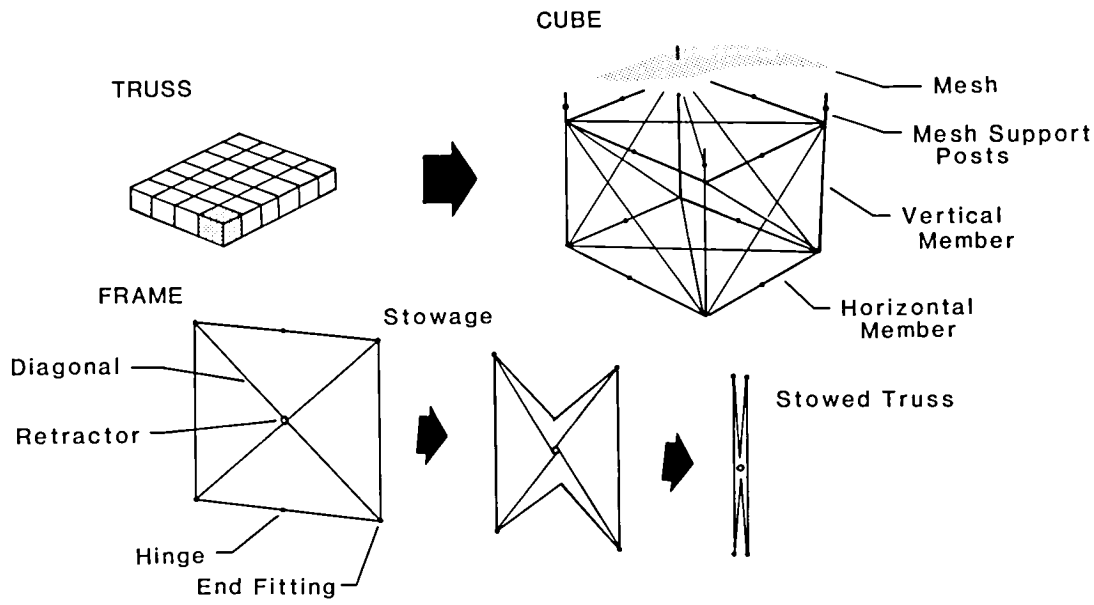

Figure 6. Box truss modular element.

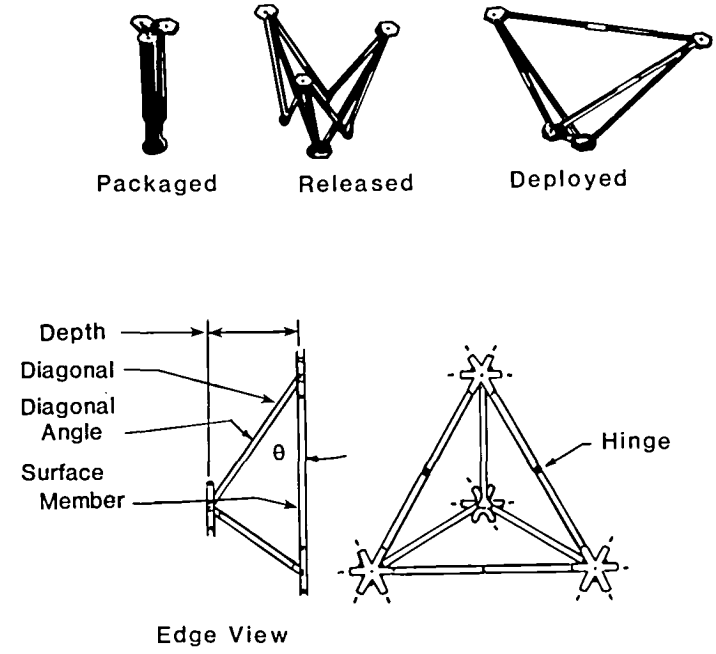

Figure 7. Tetrahedral truss modular element.

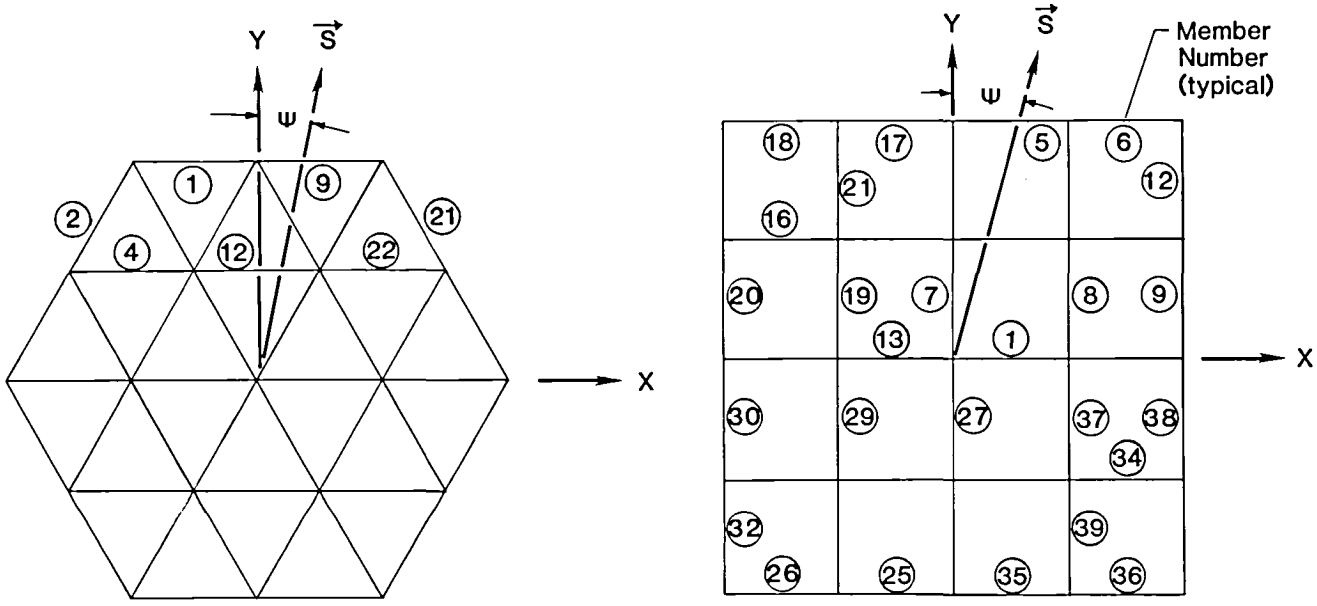

Figure 8. Orientation of solar vector $\vec{S}$ relative to TT and BT structures.

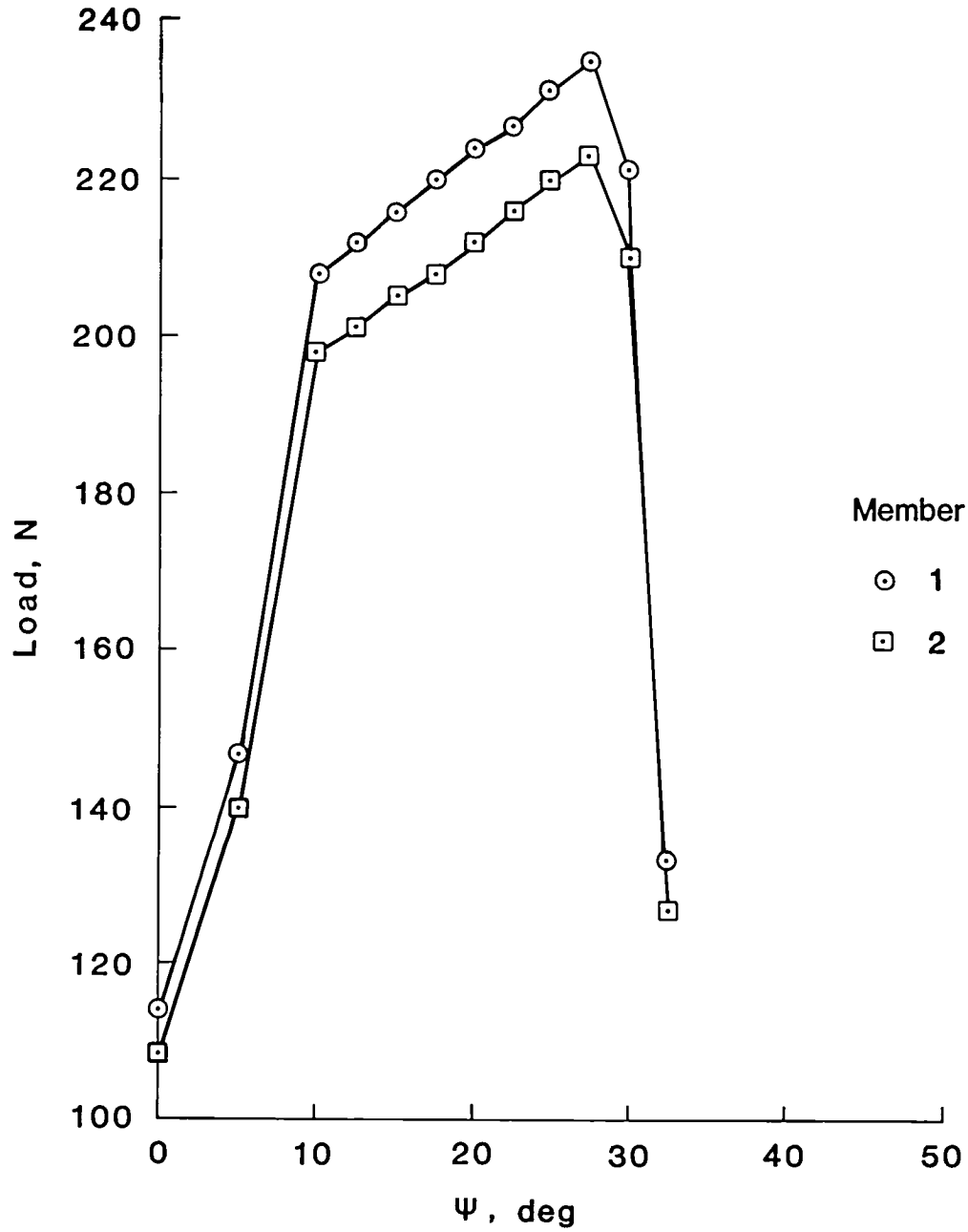

Figure 9. Changes in thermal loading on TT structure with varying incidence of solar radiation. $\Omega = 90°$; nadir-pointing Z-axis.

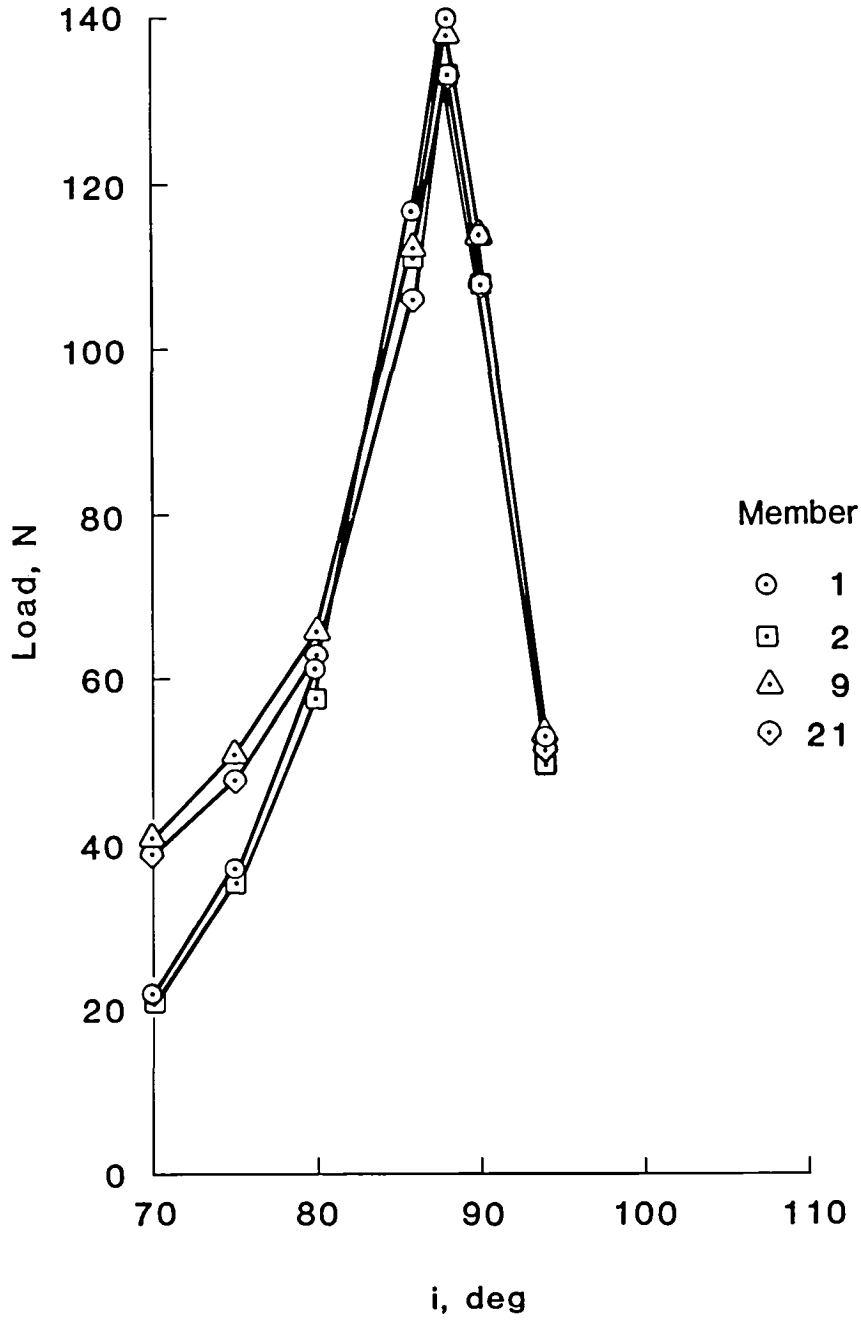

Figure 10. Changes in thermal loading on TT structure with varying inclination i. $\Omega = 90°$.

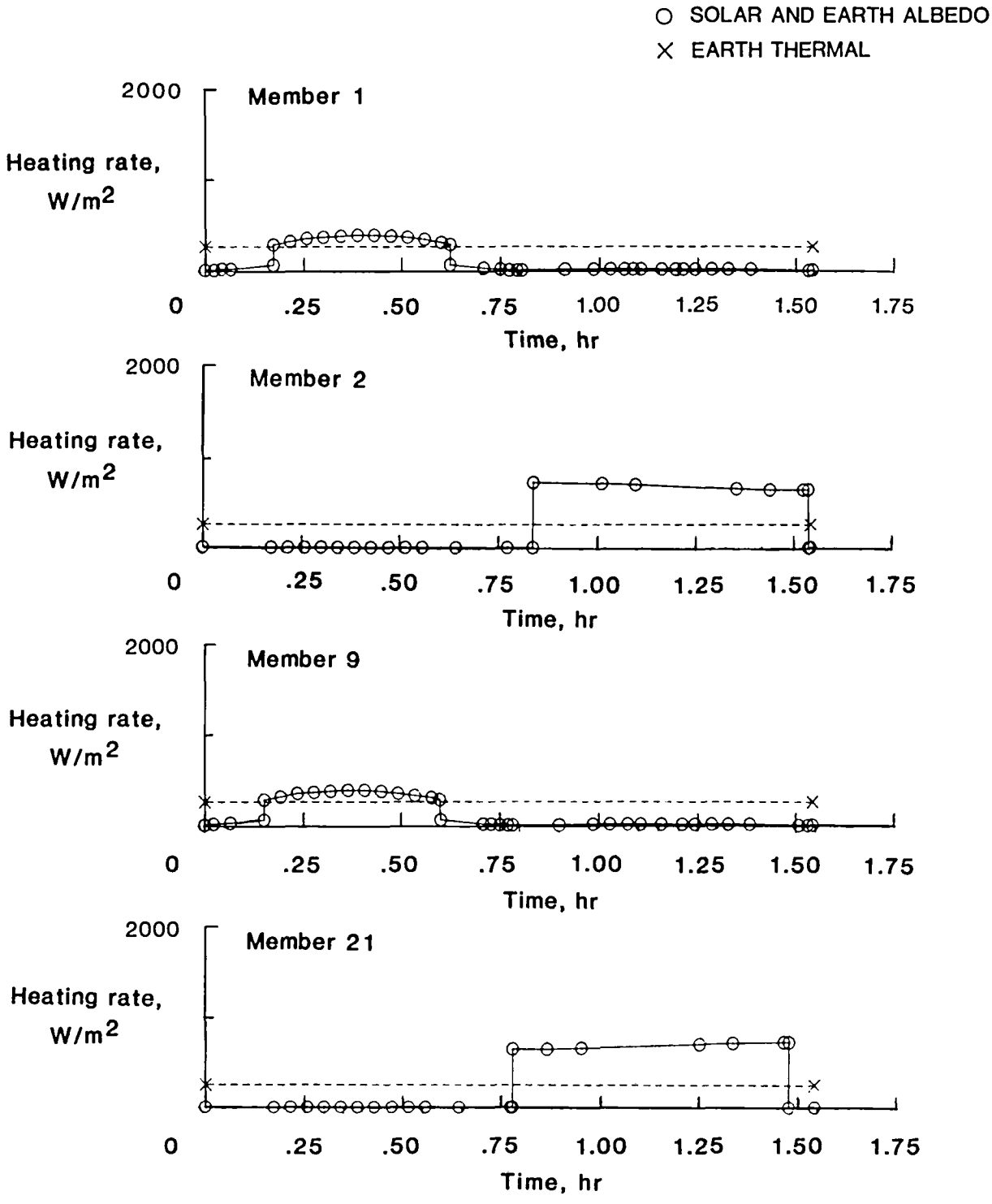

Figure 11. Heating rates for $\beta = 0°$ and $i = 88°$.

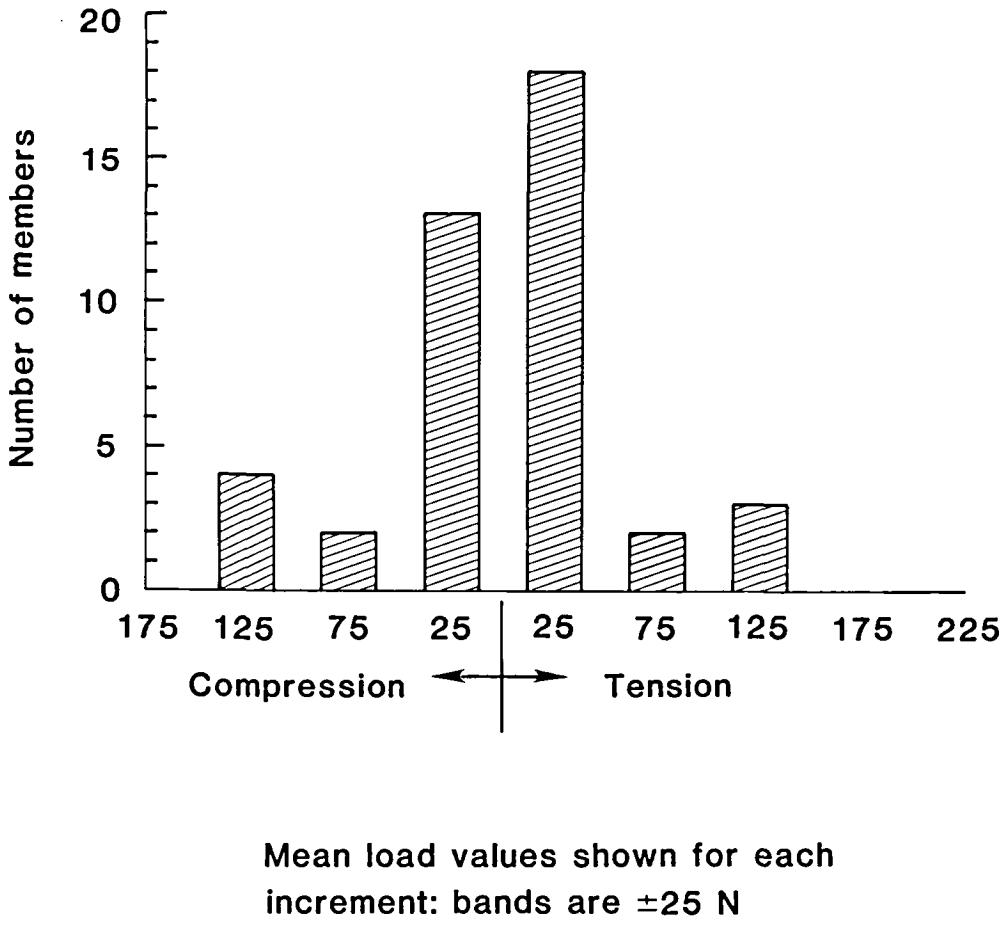

Figure 12. Tetrahedral truss front member load distributions for nominal case.

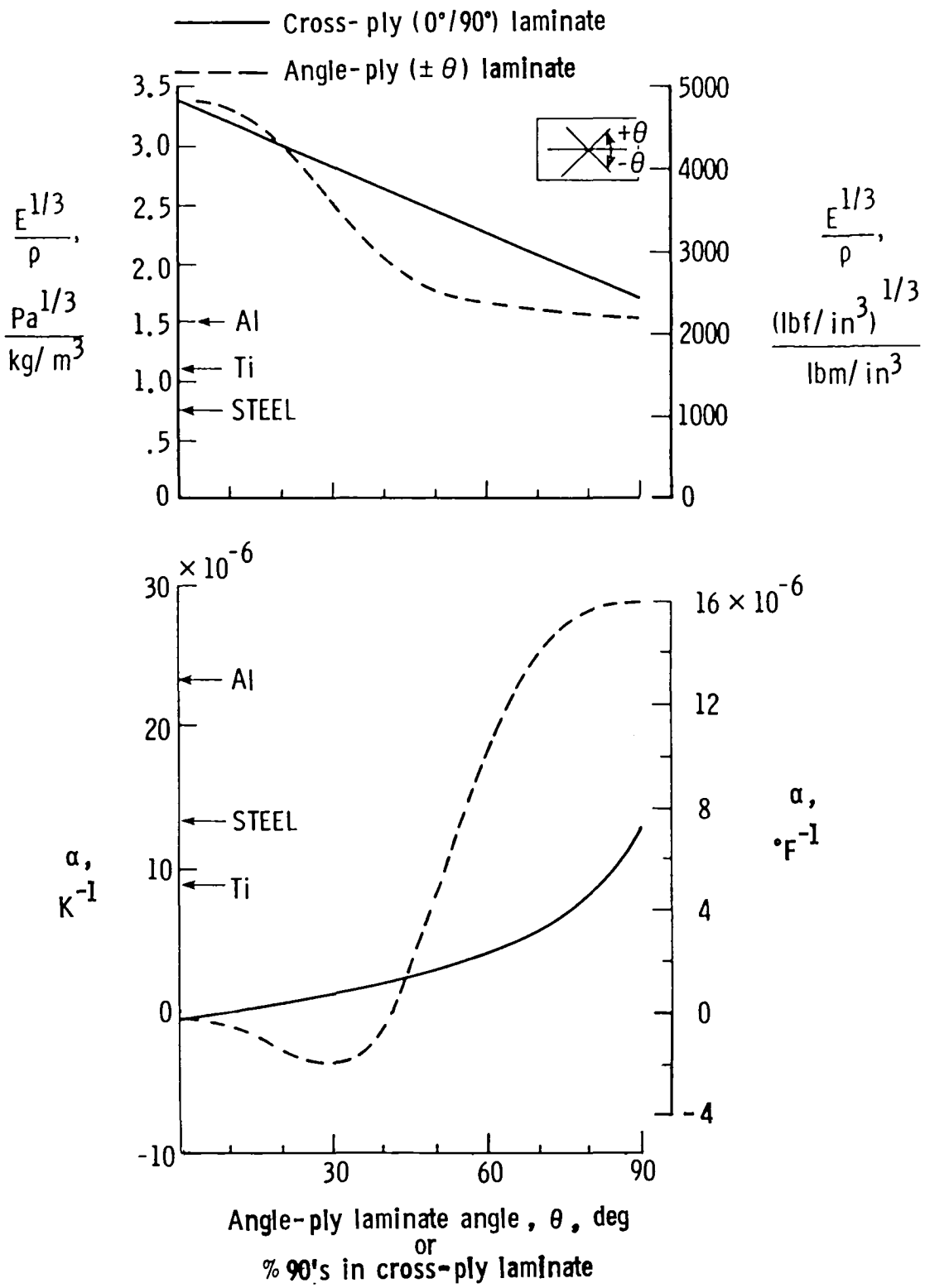

Figure 13. Material stiffness parameter and α characteristics of graphite/epoxy for two types of laminates. (From ref. 3.)

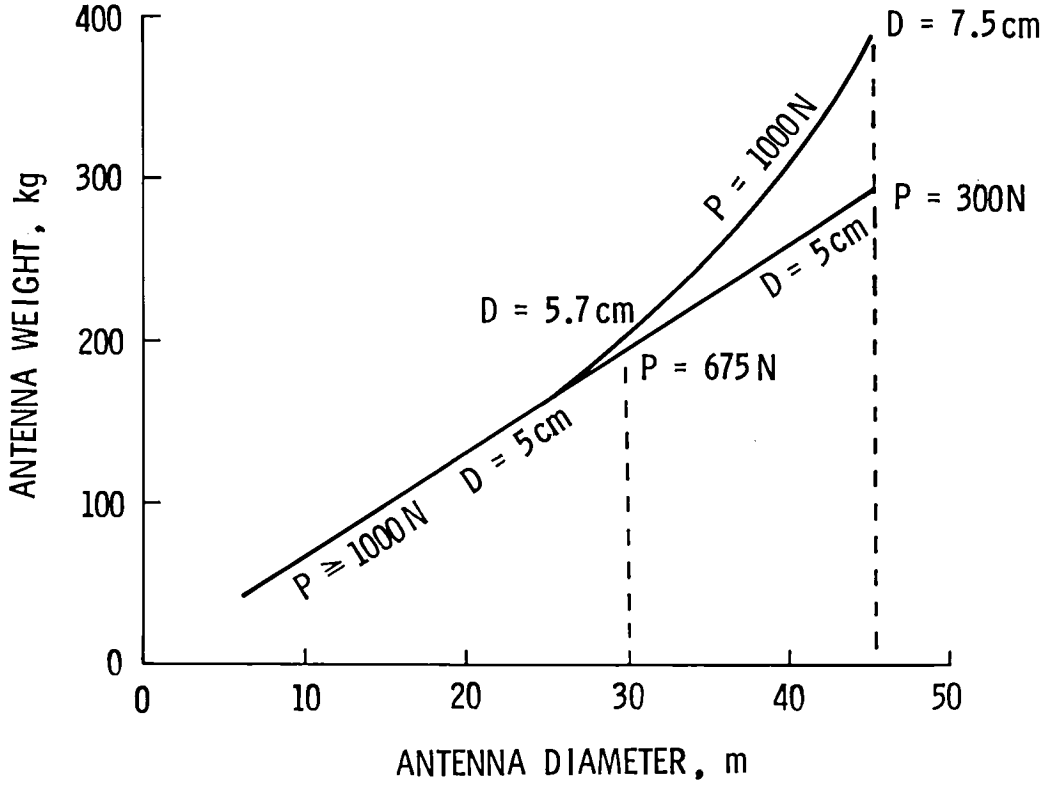

Figure 14. Tetrahedral truss antenna weight with constant tube wall thickness of 0.75 mm.

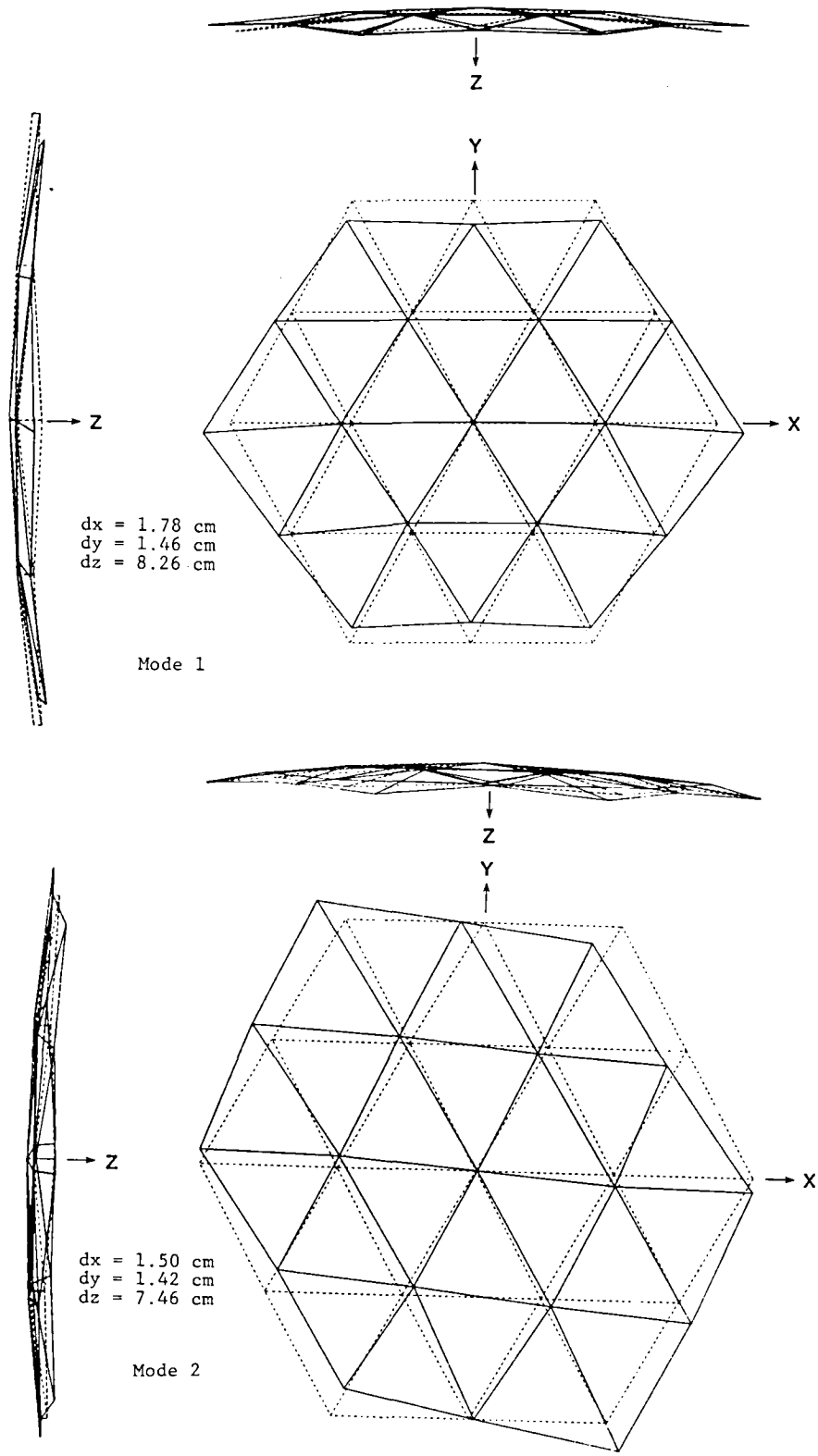

Figure 15. Mode shapes for free tetrahedral 15-m-diameter STAS.

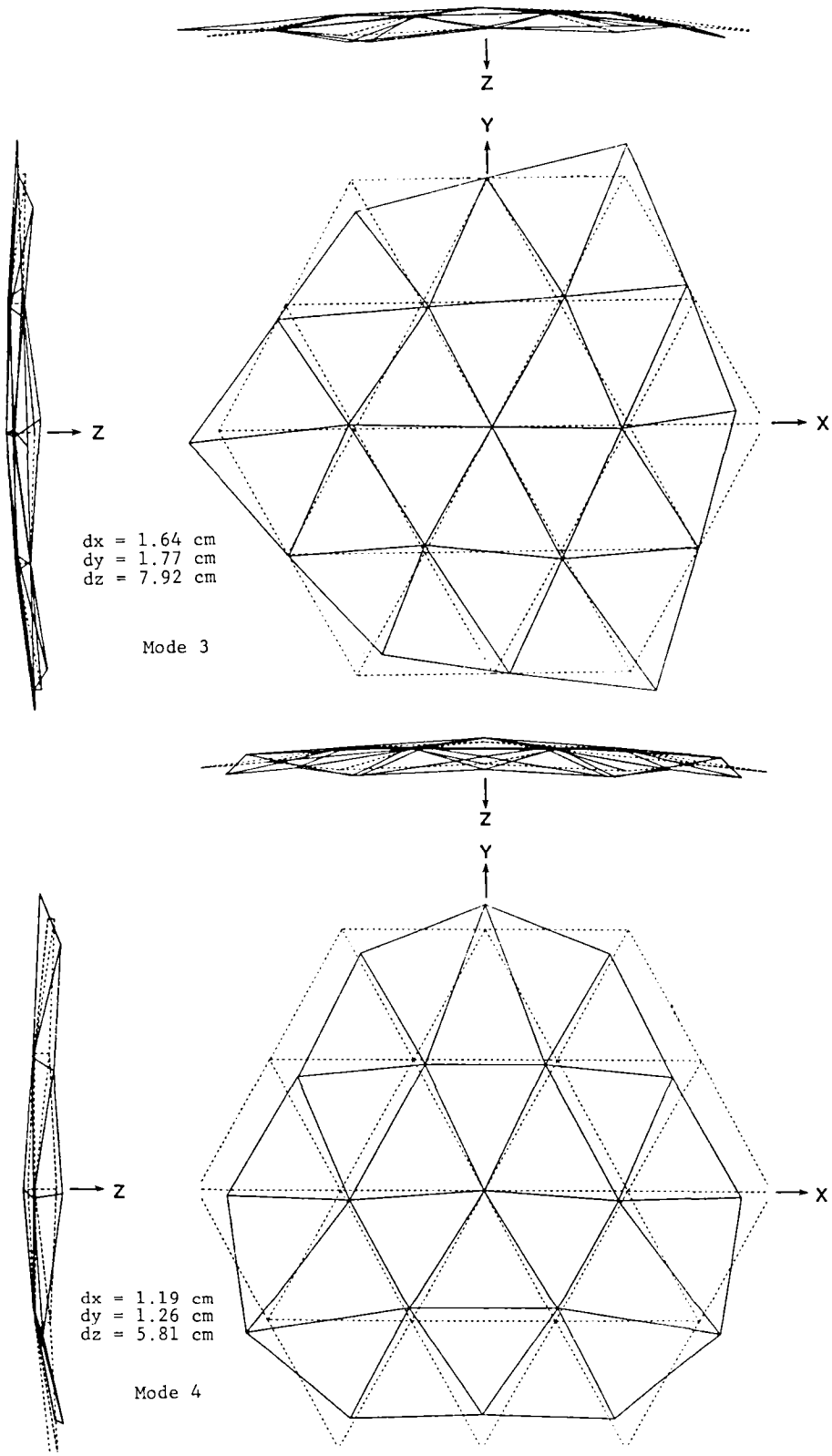

Figure 15. Continued.

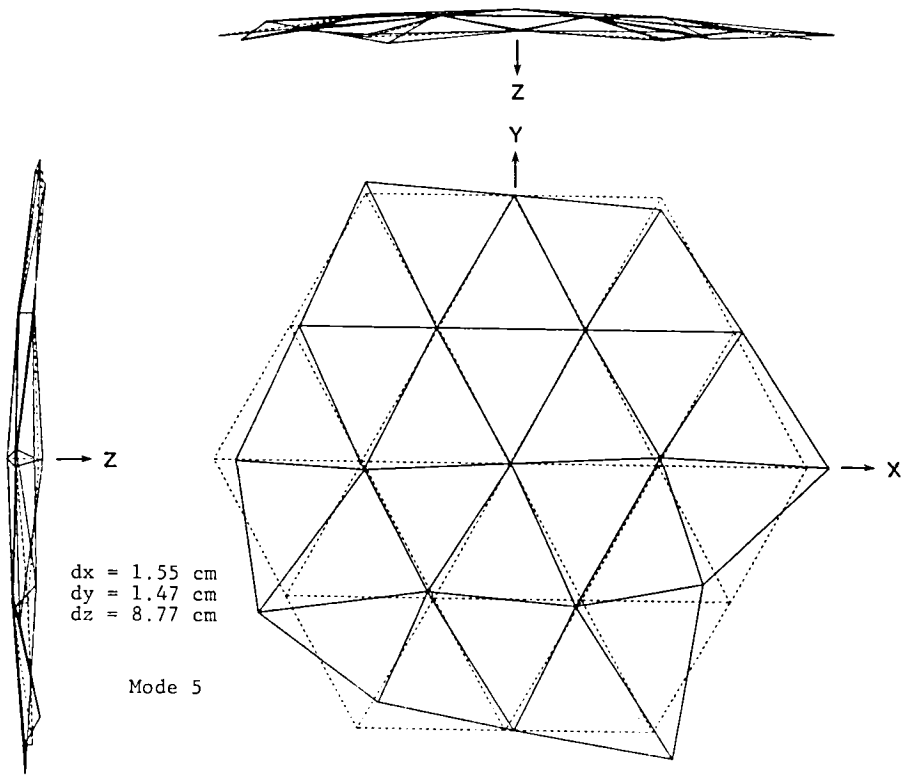

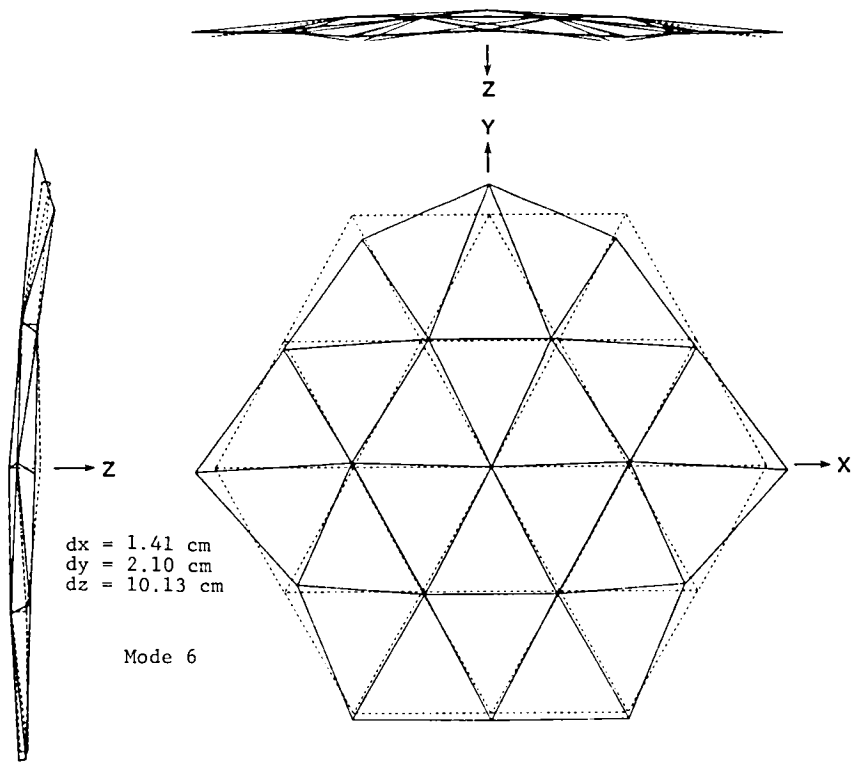

Figure 15. Concluded.

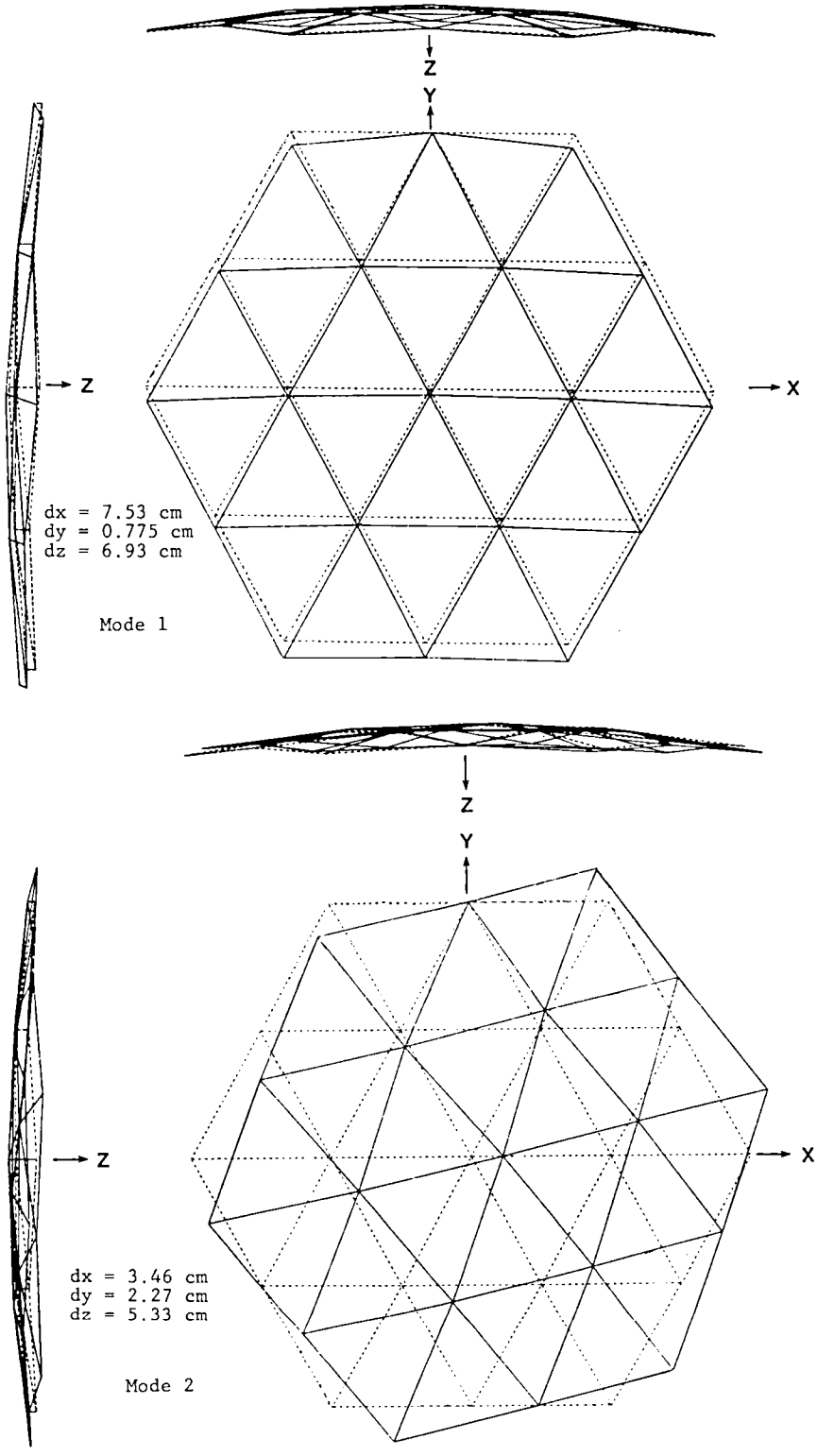

Figure 16. Mode shapes for clamped tetrahedral 15-m-diameter STAS.

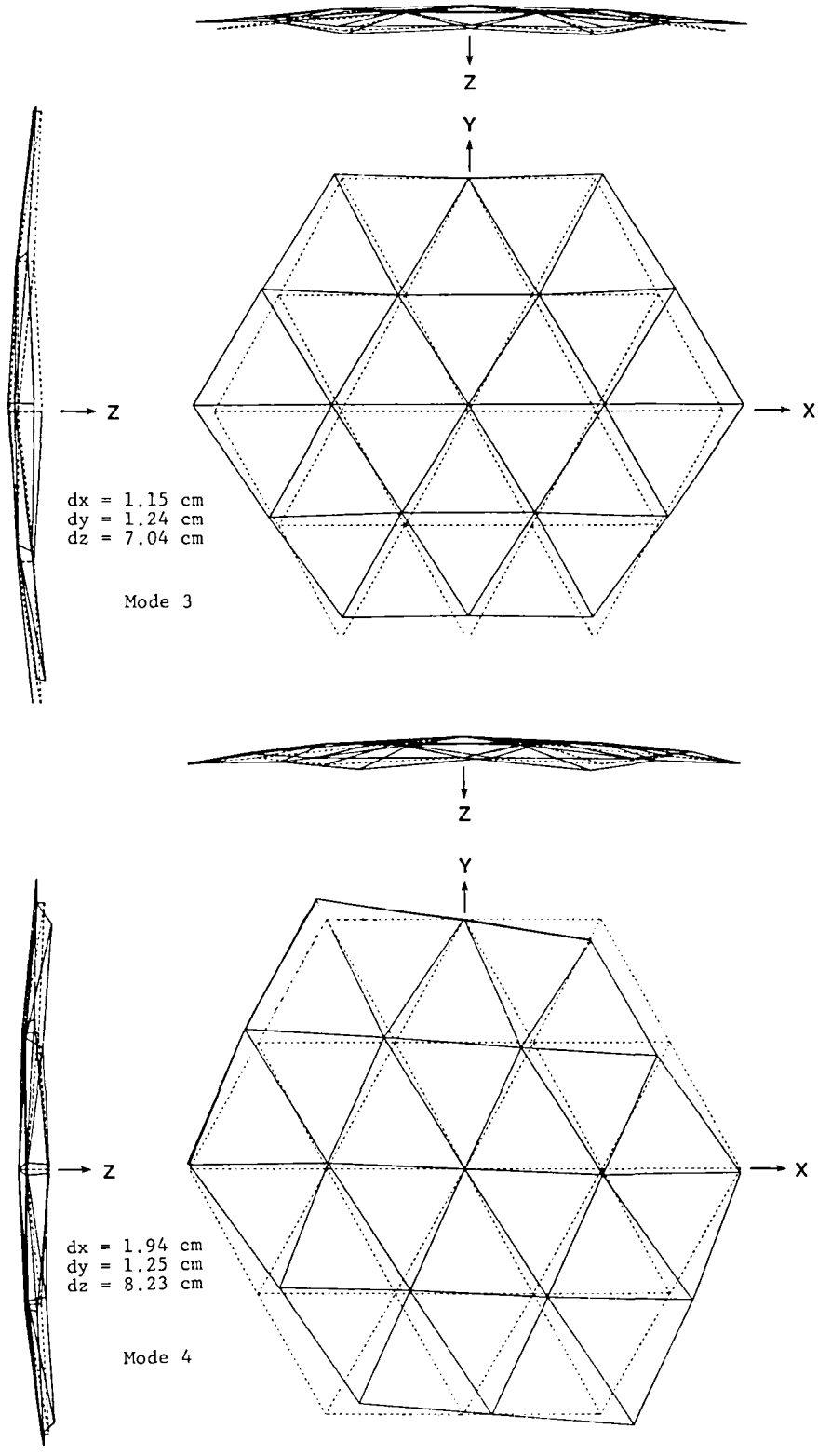

Figure 16. Continued.

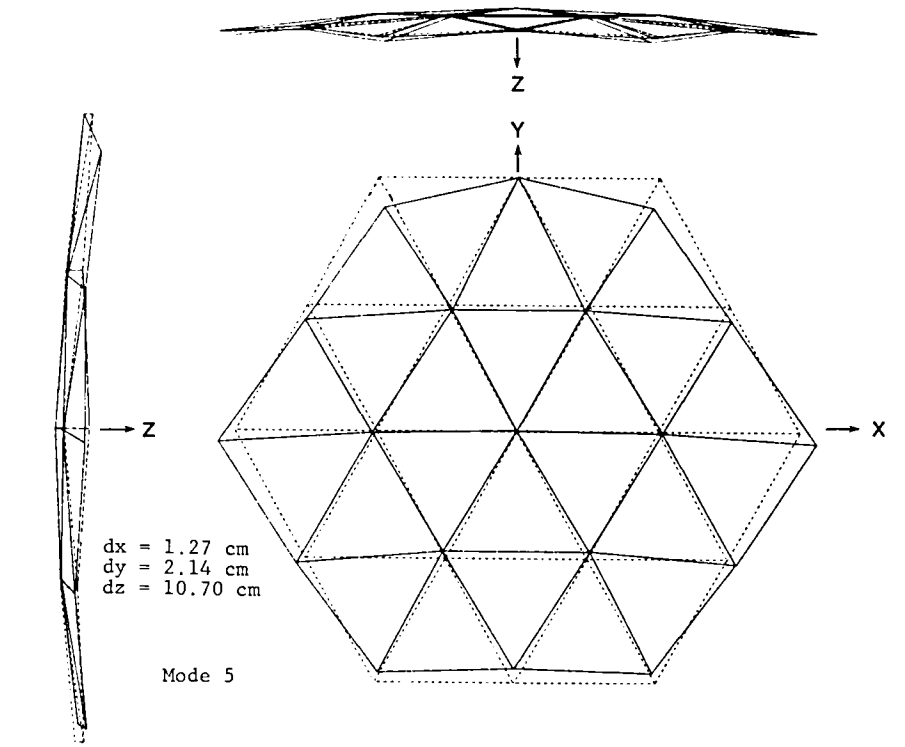

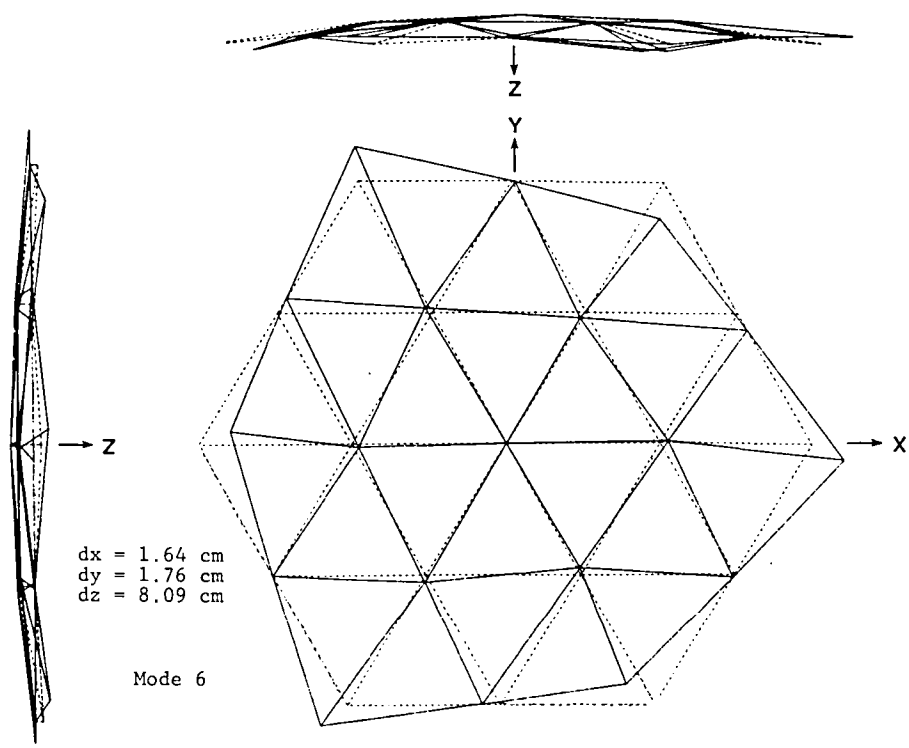

Figure 16. Concluded.

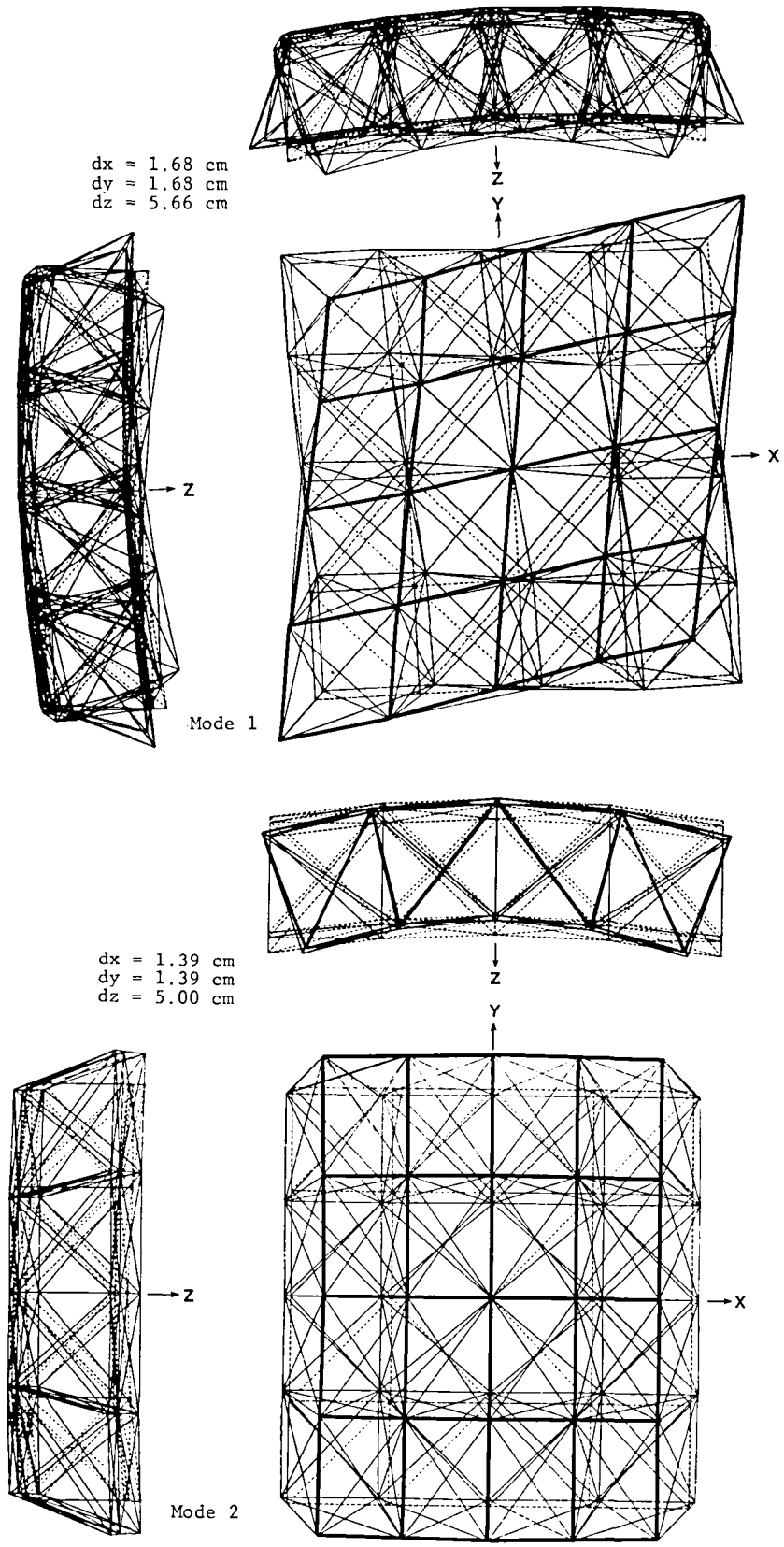

Figure 17. Mode shapes for free box truss 15-m-diameter STAS.

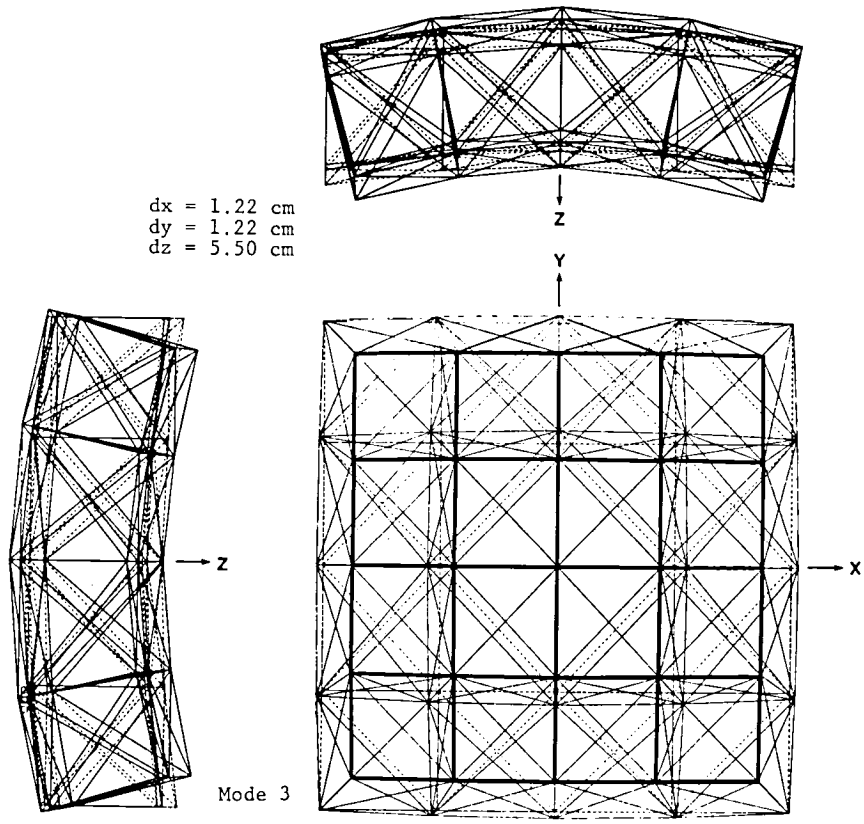

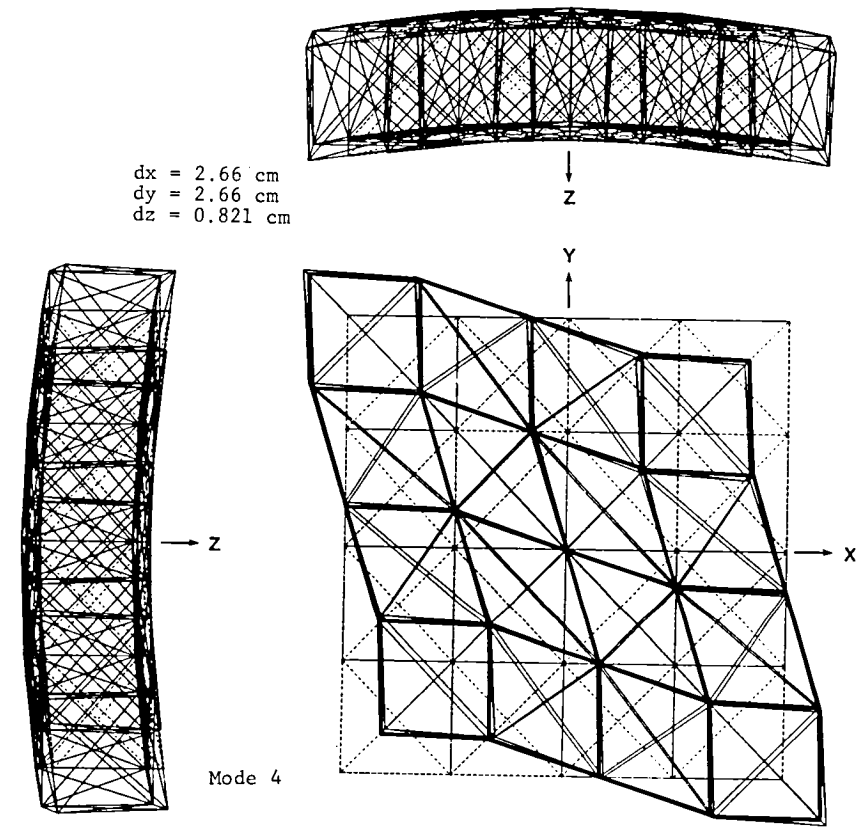

Figure 17. Continued.

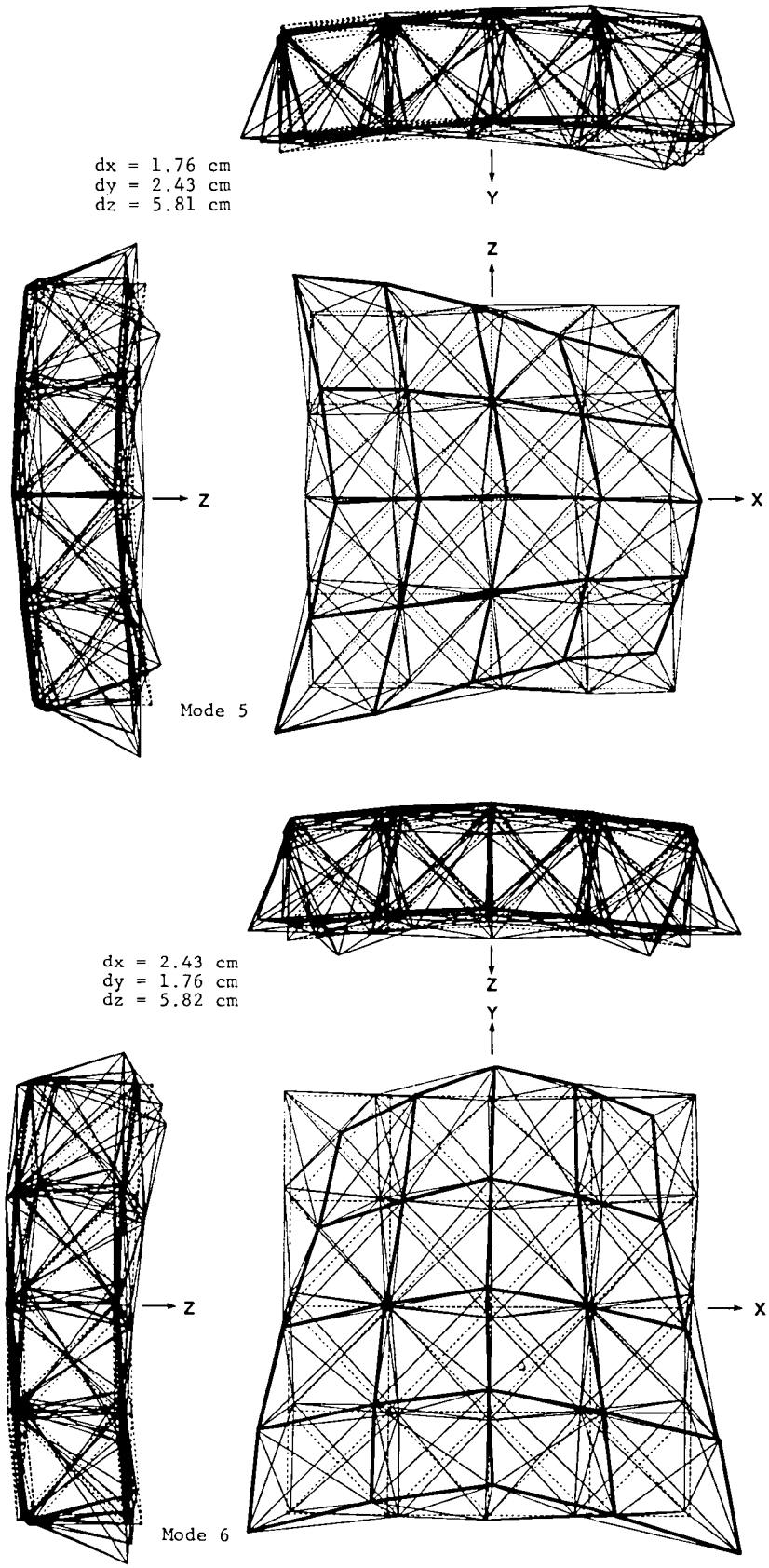

Figure 17. Concluded.

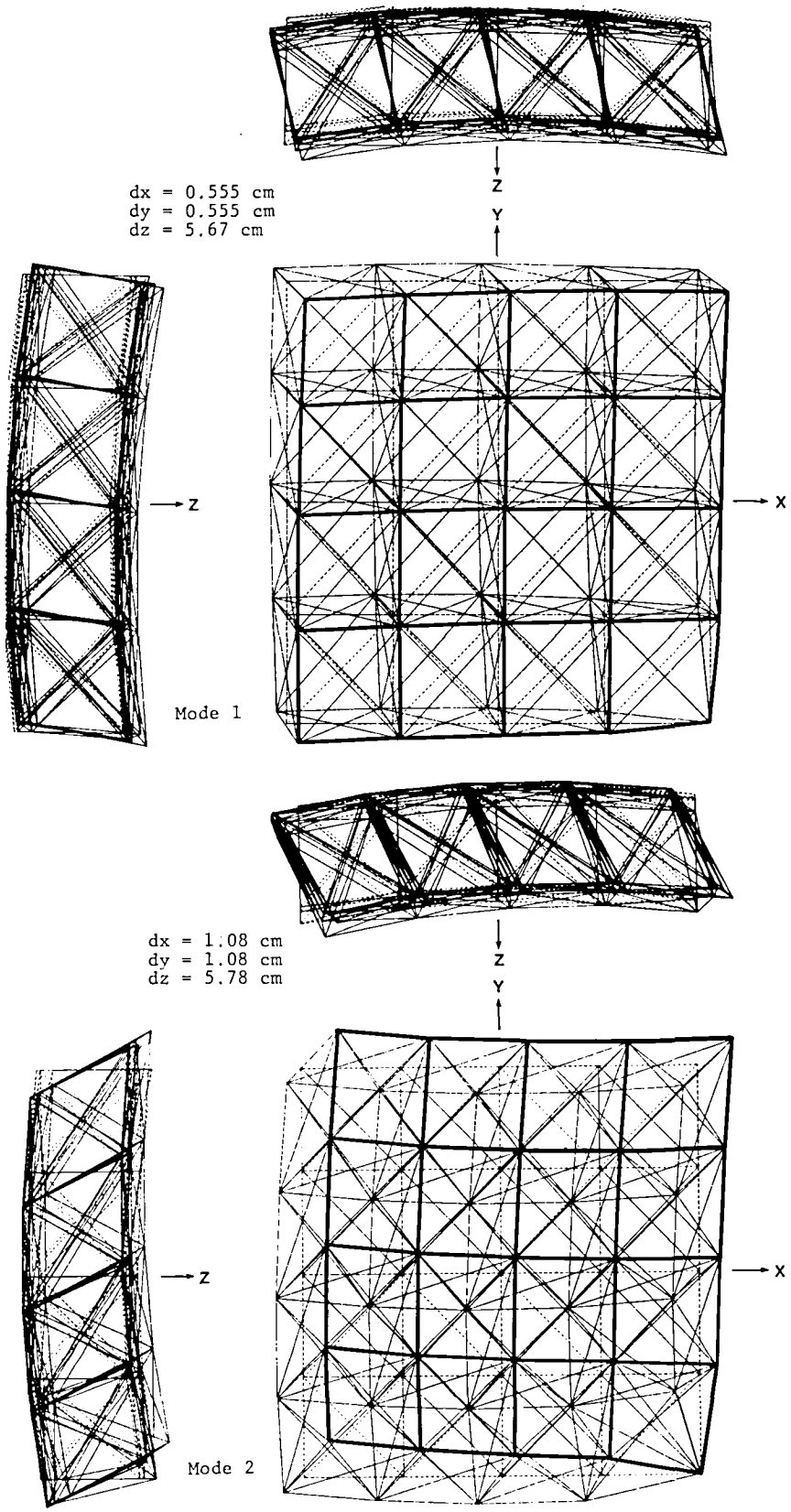

Figure 18. Mode shapes for clamped box truss 15-m-diameter STAS.

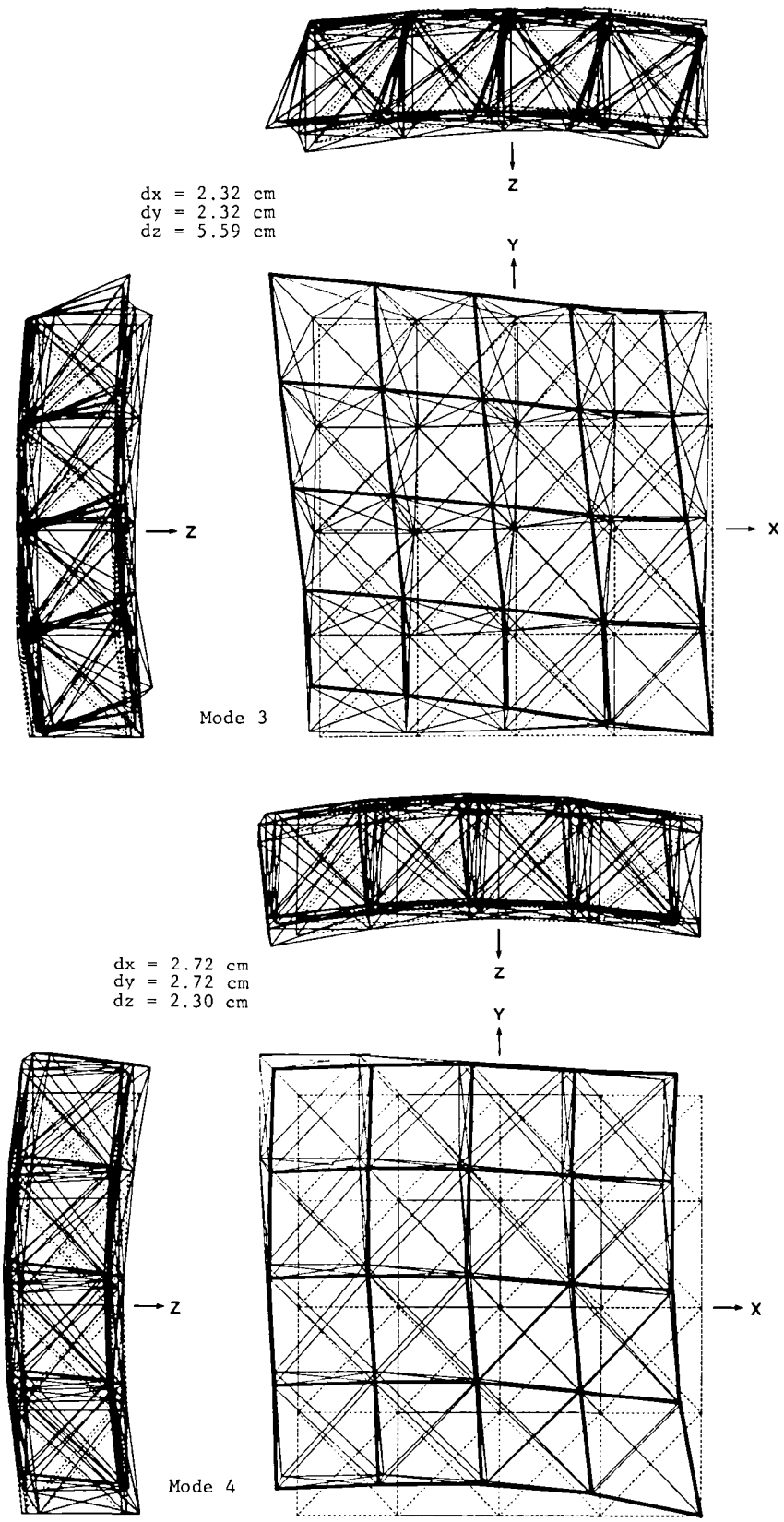

Figure 18. Continued.

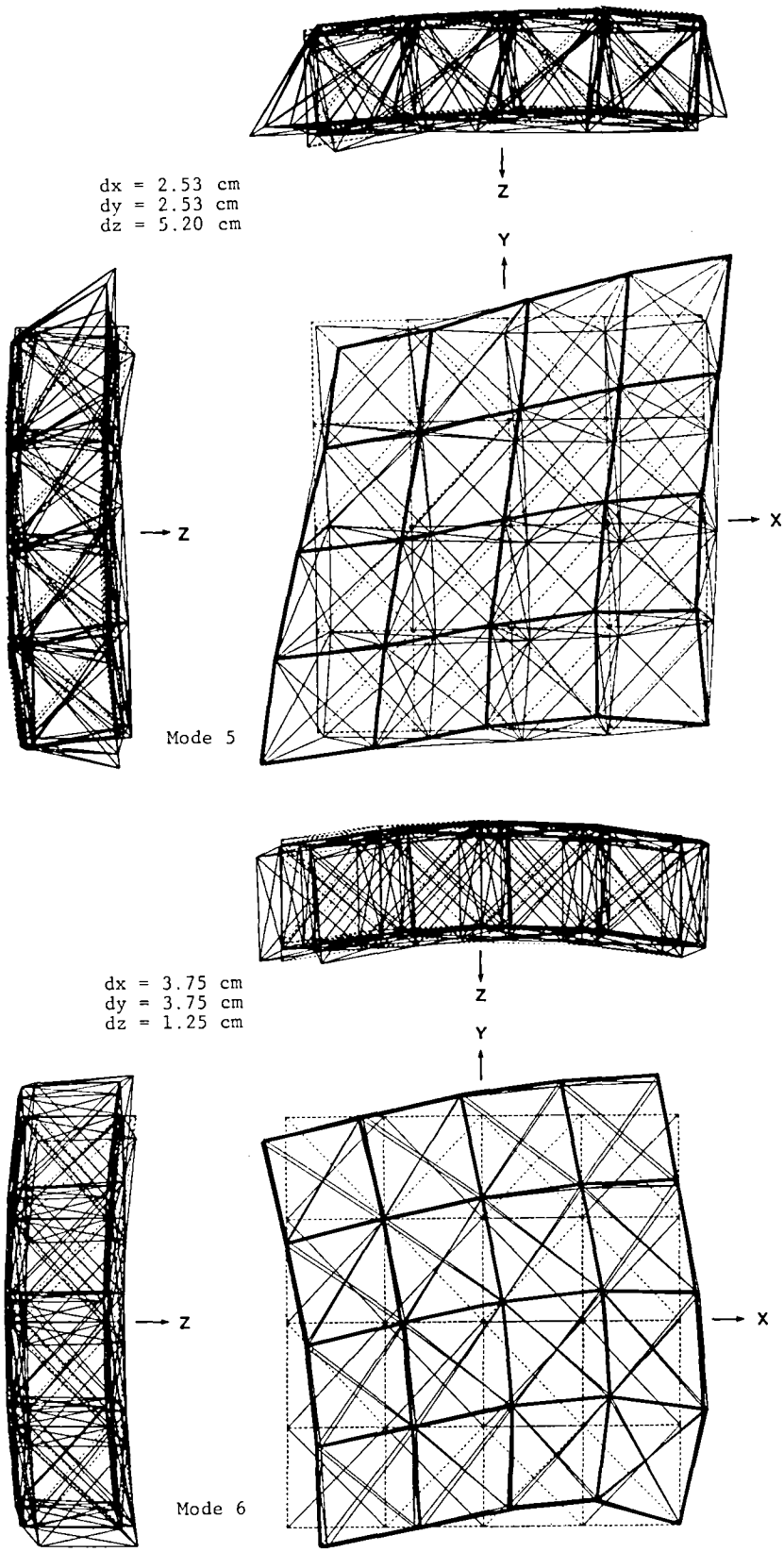

Figure 18. Concluded.

1. Report No.	2. Government Accession No.	3. Recipient's Catalog No.
NASA TM-85804		

4. Title and Subtitle	5. Report Date
CONCEPTUAL DESIGN FOR SCALED TRUSS ANTENNA FLIGHT EXPERIMENT	November 1984
	6. Performing Organization Code: 506-62-23-01
7. Author(s): Wendell H. Lee	8. Performing Organization Report No.: L-15838
9. Performing Organization Name and Address: NASA Langley Research Center, Hampton, VA 23665	10. Work Unit No.
	11. Contract or Grant No.
12. Sponsoring Agency Name and Address: National Aeronautics and Space Administration, Washington, DC 20546	13. Type of Report and Period Covered: Technical Memorandum
	14. Sponsoring Agency Code

15. Supplementary Notes

16. Abstract

The conceptual design for a Scaled Truss Antenna Structures Experiment Program (STASEP) is presented. The hardware analysis of the Scaled Truss Antenna Structure (STAS) was performed by using the Interactive Design and Evaluation of Advanced Spacecraft (IDEAS) computer-aided, interactive, design and analysis program. Four STAS's were designed—6- and 15-m-diameter tetrahedral truss and 6- and 15-m-diameter box truss antenna dishes—to be launched by the Shuttle, tested by using the Space Technology Experiments Platform (STEP) and Space Transportation System (STS), and then free flown in short lifetime orbits. Data could be gathered on deployment, structural characteristics, geometric accuracies, and thermal performance, as well as drag and lifetime as an orbiting spacecraft. All STAS's will be constructed from graphite/epoxy tubes, 5 cm in diameter with a wall thickness of 0.75 mm, and connected by hinges and end fittings. A radio frequency (RF) mesh will be mounted and integrated with the structure, and will form a parabolic antenna surface when STAS is deployed. Structural and thermal properties have been determined for the STAS, including mass properties, thermal loading, structural natural frequencies, and mode shapes. A discussion of the necessary analysis, scaling, and ground testing is included.

17. Key Words (Suggested by Authors(s))	18. Distribution Statement
Flight experiments Large space systems Conceptual design	Unclassified—Unlimited Subject Category 18

19. Security Classif.(of this report)	20. Security Classif.(of this page)	21. No. of Pages	22. Price
Unclassified	Unclassified	40	A03

For sale by the National Technical Information Service, Springfield, Virginia 22161

NASA-Langley, 1984

National Aeronautics and
Space Administration

Washington, D.C.
20546

Official Business
Penalty for Private Use, $300

THIRD-CLASS BULK RATE

Postage and Fees Paid
National Aeronautics and
Space Administration
NASA-451

NASA

POSTMASTER: If Undeliverable (Section 158
Postal Manual) Do Not Return